Received: 30 July 2018 | Accepted: 8 January 2019

DOI: 10.1111/gcb.14570

PRIMARY RESEARCH ARTICLE

WILEY Global Change Biology

Effects of anthropogenic nitrogen discharge on dissolved inorganic nitrogen transport in global rivers

Shuang Liu[1,2] | Zhenghui Xie[1,3] | Yujin Zeng[4] | Bin Liu[1,3] | Ruichao Li[1,3] | Yan Wang[1,3] | Longhuan Wang[1,3] | Peihua Qin[1] | Binghao Jia[1] | Jinbo Xie[1]

[1]State Key Laboratory of Numerical Modeling for Atmospheric Sciences and Geophysical Fluid Dynamics, Institute of Atmospheric Physics, Chinese Academy of Sciences, Beijing, China

[2]Key Laboratory of Mountain Hazards and Earth Surface Processes, Institute of Mountain Hazards and Environment, Chinese Academy of Sciences, Chengdu, China

[3]University of Chinese Academy of Sciences, Beijing, China

[4]Program in Atmospheric and Oceanic Sciences, Princeton University, Princeton, New Jersey

Correspondence
Zhenghui Xie, State Key Laboratory of Numerical Modeling for Atmospheric Sciences and Geophysical Fluid Dynamics, Institute of Atmospheric Physics, Chinese Academy of Sciences, Beijing, China.
Email: zxie@lasg.iap.ac.cn

Funding information
Key Research Program of Frontier Sciences, Chinese Academy of Sciences, Grant/Award Number: QYZDY-SSW-DQC012; National Natural Science Foundation of China, Grant/Award Number: 41830967 and 41575096

Abstract

Excess nutrients from fertilizer application, pollution discharge, and water regulations outflow through rivers from lands to oceans, seriously impacting coastal ecosystems. A reasonable representation of these processes in land surface models and River Transport Models (RTMs) is very important for understanding human–environment interactions. In this study, the schemes of riverine dissolved inorganic nitrogen (DIN) transport and human activities including nitrogen discharge and water regulation, were synchronously incorporated into a land surface model coupled with a RTM. The effects of anthropogenic nitrogen discharge on the DIN transport in rivers were studied based on simulations of the period 1991–2010 throughout the entire world, conducted using the developed model, which had a spatial resolution of about 1° for land processes and 0.5° for river transport, and data on fertilizer application, point source pollution, and water use. Our results showed that rivers in western Europe and eastern China were seriously polluted, on average, at a rate of 5,000–15,000 tons per year. In the Yangtze River Basin, the amount of point source pollution in 2010 was about four times more than that in 1991, while the amount of fertilizer used in 2010 doubled, which resulted in the increased riverine DIN levels. Further comparisons suggested that the riverine DIN in the USA was affected primarily by nitrogen fertilizer use, the changes in DIN flow rate in European rivers was dominated by point source pollution, and rivers in China were seriously polluted by both the two pollution sources. The total anthropogenic impact on the DIN exported to the Pacific Ocean has increased from 10% to 30%, more significantly than other oceans. In general, our results indicated that incorporating the schemes of nitrogen transport and human activities into land surface models could be an effective way to monitor global river water quality and diagnose the performance of the land surface modeling.

KEYWORDS

earth system model, global biogeochemical cycle, human activities, land surface model, riverine nitrogen transport, water pollution

1 | INTRODUCTION

Nutrient transfer and transport in soil and rivers support the development of biocenosis and connect the ecosystems between land and oceans, which are important for offshore environments and global biogeochemical cycles (BGCs) (Jickells, 1998). In recent decades, through the anthropogenic nitrogen discharge from activities such as fertilizer application, fossil fuel consumption, and leguminous crop production, the amount of biologically available nutrients entering the terrestrial ecosystem has more than doubled in comparison to

preindustrial era levels (Galloway et al., 2004). Humans have also greatly altered global hydrological systems by extracting groundwater and water from major rivers (Haddeland et al., 2014; Pokhrel, Hanasaki, Wada, & Kim, 2016; Zeng, Xie, & Zou, 2017). For example, irrigation can result in an increase in soil nitrogen leaching (Woli, Hoogenboom, & Alva, 2016), while dams can inadvertently detain considerable nutrients that would otherwise be carried by rivers to oceans (Maavara et al., 2015; Van Cappellen & Maavara, 2016). These changes in both the global nutrient and hydrological cycles have effects on the earth system, and are the cause of some environmental problems such as offshore marine pollution (Bouwman, Beusen, & Billen, 2009; Bouwman et al., 2011). Quantifying riverine nutrient transport and its response to human activities is important toward understanding how the global environment evolves, the connection between land and seas, and the interaction between social development and natural ecosystems.

Numerical models have been widely used to simulate nutrient transfer from lands to oceans (Seitzinger, Harrison, Dumont, Beusen, & Bouwman, 2005; Seitzinger et al., 2010; Seitzinger & Phillips, 2017). Initial models considered the relationships between nutrient loads and their concentration at river mouths, which have been used to estimate the amount of exported nutrients by rivers at basin scales (Boyer et al., 2006; Howarth, 1998; Peierls, Caraco, Pace, & Cole, 1991). Subsequent models further considered the impact of river length, nutrient decomposition, and sedimentation (Alexander et al., 2009; Arnold & Fohrer, 2005; Wollheim, Peterson, Thomas, Hopkinson, & Vörösmarty, 2008). However, these models were not applied at global scales. Hence, the Global Nutrient Export from Watersheds (Global NEWS) work group, which belongs to UNESCO-IOC (United Nations Educational, Scientific and Cultural Organization - Intergovernmental Oceanographic Commission), established predictive, multiform models of riverine nutrient export (Seitzinger et al., 2010). The Global NEWS models simulated the global riverine export of dissolved inorganic nitrogen (DIN), phosphorus, and silica (DIN, DIP, and DIS, respectively), dissolved organic carbon, nitrogen, and phosphorus (DOC, DON, and DOP, respectively), and particulate organic carbon, nitrogen, and phosphorus (POC, PN, and PP, respectively) (Beusen, Bouwman, Dürr, Dekkers, & Hartmann, 2009; Beusen, Dekkers, Bouwman, Ludwig, & Harrison, 2005; Harison et al., 2005; Mayorga et al., 2010). Most of these large-scale studies treated river basins as the basic unit so that detailed information of nitrogen leaching or riverine nitrates in distributed grids was lacking. To address this, He et al. (2011) used a spatially explicit BGC modeling framework, which was established by unidirectionally linking a land surface model (Surface Interaction and Runoff Model, MATSIRO) with a terrestrial nitrogen cycle model to assess global nitrogen pollution. Beusen, Beek, Bouwman, Mogollón, and Middelburg (2015) also combined the IMAGE (Integrated Model to Assess the Global Environment) with a distributed hydrological model to simulate global nutrient transportation. Although these works expended considerable efforts by connecting individually calibrated models in series, the models still could not describe the interaction between hydrological and ecological processes. More importantly, these hydrological models are not easily coupled with the earth system models with regard to comprehensive global BGC modeling. In order to address these issues, Nevison, Hess, Riddick, and Ward (2016) performed a preliminary investigation where they coupled nitrogen leaching and runoff flow rates from the Community Land Model (CLM) to the River Transport Model (RTM) within the Community Earth System Model (CESM) to simulate riverine nitrogen transport.

Key Points

- A riverine nitrogen transport model that considers river water temperature change, anthropogenic nitrogen discharge, water regulation, and interactions between hydrological and ecological processes was developed.
- Riverine dissolved inorganic nitrogen (DIN) in the USA has increased primarily due to the use of nitrogen fertilizers. In contrast, European rivers were affected mainly by point source pollution. Both aspects are equally important for aquatic environments in China.
- The impact of anthropogenic nitrogen discharge on the DIN exported to the Pacific Ocean grew most significantly from 1991 to 2010.

Current descriptions of riverine nutrient transport in land surface models within the earth system model frameworks are incomprehensive as they neglect the impact of related human activities. To address this issue, in this work we considered DIN as a case study, and the schemes of global riverine nutrient transport with dynamic water temperature, anthropogenic water regulation, and nitrogen discharge were synchronously incorporated into a land surface model. Then, using a series of data related to fertilizer applications, point source pollution, surface water, and groundwater use, numerical simulations for the period 1991–2010, which had an approximate 1° spatial resolution for land processes and 0.5° resolution for river systems, were conducted for the entire globe to explore the impact of anthropogenic nitrogen discharge on riverine DIN transport from land to oceans.

2 | MATERIALS AND METHODS

2.1 | Model development

2.1.1 | Land surface model and a scheme for soil nitrogen transport to rivers

The community land model CLM4.5 (Oleson et al., 2013) was used as the base model for the model development in this work. It was developed by the National Center for Atmospheric Research, and it is the land surface component of the Community Earth System Model (CESM1.2.0) (Hurrell et al., 2013). The model CLM4.5 includes biogeophysical (BGP) and BGC mechanisms, and energy and mass flow

rates from the land to the atmosphere. BGC processes including vegetation photosynthesis, phenology, the carbon and nitrogen cycles, decomposition, and wildfires are represented in CLM4.5 (Lindsay et al., 2014). CLM4.5 also contains an interactive crop management model, which simulates temperate crop growth with nitrogenous fertilizer application. CLM4.5 uses a sub-grid hierarchy of land units, soil profiles, and plant function types to describe the heterogeneity within each grid cell. Different land uses, such as varieties of vegetation, lakes, urban areas, and glaciers, are addressed separately even if they coexist in a given grid cell.

In the model, the input of new mineral nitrogen comes from atmospheric deposition, biological nitrogen fixation, and fertilizer application. Losses of mineral nitrogen are due to nitrification, denitrification, leaching, and fires. Among these aspects, most of the nitrogen leaching should be carried by water flowing from land to oceans. In the model, the nitrogen leaching calculations consider soil DIN runoff by surface runoff and DIN leaching by subsurface drainage. The general equation is written as follows:

$$X_N = \frac{Q_x NS_{sminn}}{WS_{soil}}, \quad (1)$$

where X_N denotes the soil DIN runoff or leaching, Q_x means the surface runoff or subsurface runoff, NS_{sminn} is the nitrogen storage in soil mineral nitrogen pools, and WS_{soil} is the water storage in soil. The nitrogen loss rate depends on the concentration of dissolved mineral nitrogen in soil water solutions. In this work, we adopted the Century-based formulation within CLM4.5, in which the leaching acts only on NO_3^- pools, while NH_4^+ pools were assumed to be 100% adsorbed onto mineral surfaces and are hence unaffected by leaching. Equation 1 is a general expression, which shows the basic idea of soil DIN runoff and leaching in CLM4.5. The actual calculation of soil DIN runoff and leaching is more complex than that shown in Equation 1. In the specific code for the BGC module of CLM4.5, the DIN concentration in each soil layer is calculated based on the volume content of soil mineral NO_3^-, the corresponding layer thickness and the liquid water content in each soil layer. Then the DIN leaching rate in each soil layer is calculated using each DIN concentration and the sub-surface drainage flux in each layer, which is estimated based on the amount of liquid water in each soil layer, the corresponding layer thickness and the total liquid water in each soil column. Analogously, the DIN runoff rate in each layer is calculated using each DIN concentration as well, and the surface runoff flux, which is estimated based on the amount of liquid water in each soil layer, the corresponding layer thickness and the total soil liquid water to shallow surface depth. However, it is still difficult to know where the modelled soil nitrogen runoff and leaching will go in the river transport systems in the current version of CLM4.5.

2.1.2 | A scheme for riverine nitrogen transport

The RTM in CLM4.5 was developed to route the total runoff from the land to oceans or marginal seas, which enables the hydrologic cycle to be closed (Branstetter & Erickson, 2003). It also provides another method for diagnosing the performance of the land model because the river flow can be directly compared to actual station data. The RTM uses a linear transport scheme to route water from each grid cell to its downstream neighboring grid cell. The flow direction of each cell is determined based on the steepest slope.

Based on the water transport framework, we treated the DIN inputs, including soil DIN runoff and leaching, nitrogen deposition, and point source nitrogen discharge, as tracers, and then constructed an equation for the large-scale riverine nitrogen transport:

$$\frac{dS_N}{dt} = \sum F_{N,in} - F_{N,out} + Runoff_N + Leaching_N + Pollution_N + Deposition_N - Loss_N, \quad (2)$$

$$F_{N,out} = \frac{vS_N}{d}, \quad (3)$$

where S_N denotes the DIN storage in the current river grid cell, t is the time step for river routing, $F_{N,in}$ means the riverine DIN inflow from eight neighboring grid cells, $F_{N,out}$ means the riverine DIN outflow from the current grid cell, $Runoff_N$ is the soil DIN runoff taken away by the surface runoff, $Leaching_N$ is the soil DIN leaching through the subsurface drainage, $Pollution_N$ is the point source nitrogen pollution, which is often determined statistically or estimated from datasets, $Deposition_N$ is the nitrogen deposition from the atmosphere to the river, which is neglected in this work, $Loss_N$ is the DIN retention during the transport, which reflects any DIN losses by denitrification, sedimentation and uptake by aquatic plants, v is the effective water flow velocity, which is determined by the mean slope, and d is the distance between the centers of neighboring grid cells (Oleson et al., 2013).

Based on a previous work (Nevison et al., 2016), the DIN retention during the transport could be calculated as follows:

$$Frac = 1 - \exp\left(\frac{-e_f \tau}{h}\right), \quad (4)$$

where Frac is the fraction denitrified, τ is the residence time within the river, e_f is a biological activity coefficient for denitrifiers, and h is the depth, which is estimated as an empirical function of flow as follows (Andreadis, Schumann, & Pavelsky, 2013):

$$h = 0.27Q^{0.3}, \quad (5)$$

where Q is the river water flow. In addition, in this work, e_f could be calculated dynamically with the up-to-date river water temperature and DIN concentration, which is expressed as follows:

$$e_f = v_f \alpha^{(rt-20)} f(con), \quad (6)$$

where v_f is a constant value of 35 m/year for the biological activity coefficient (Wollheim, Vörösmarty et al., 2008), α is 1.0717 for nitrogen and f(con) is a coefficient related to the DIN concentration (Beusen et al., 2015). The term rt is the river water temperature, which is calculated based on the work of Van Vliet et al. (2012). For large-scale

applications, the advection term dominates, so the dispersion can be neglected. The water temperature is calculated for a river segment based on the upstream water temperature and inflow into the segment, the heat exchange at the air–water interface, and the inflow and temperature of water from tributaries. We also incorporated anthropogenic heat discharge from thermoelectric power plants into the model. Hence, the 1D-heat advection equation can be written as follows:

$$\frac{\partial T_w}{\partial t}\rho_w c A_x = \frac{Q_{in}\rho_w c\Delta T_{in}}{\partial x} + \frac{Q_{runoff}\rho_w c\Delta T_{runoff}}{\partial x} + H_{air\text{-}water} w_x + \frac{Q_{human}\rho_w c\Delta T_{human}}{\partial x}, \quad (7)$$

where T_w is the water temperature, ρ_w is the density of water, c is the specific heat capacity of water, ΔT_{in} is the difference between the advected temperature from upstream and the river temperature at the current location, ΔT_{runoff} is the difference between the advected temperature from runoff yield and the river temperature at the same grid cell, w_x is the stream width, x denotes the segment length, which is equal to the length of the river grid cell, ΔT_{human} is the difference between the advected temperature from human heat emission and the river temperature in the same grid cell, and Q_{human} is the water discharged from once-through cooling systems. It should be noted that the emitted heat was added to the river to warm the water, using the ready-made data provided by Raptis and Pfister (2016).

Next, $H_{air\text{-}water}$ is the dominant heat exchange at the air–water surface, which is calculated based on the stream energy balance equation of Wunderlich and Gras (1967). Based on a series of empirical equations (Hao, Li, & Zhuang, 2005; Xu, Yu, Li, & Yang, 2016), the heat exchange between air and water can be approximately expressed as follows:

$$H_{air\text{-}water} = 0.97H_{si} + 0.97\sigma\left[\varepsilon_a\left(273.15+T_a\right)^4 - \left(273.15+T_s\right)^4\right] - \mu f(\text{wind})\left(T_s - T_d\right) - 0.47f(w)\left(T_s - T_a\right), \quad (8)$$

where the terms in the right hand side of the equation are the net shortwave radiation, net longwave radiation, latent heat flux and sensible heat flux. H_{si} is solar shortwave radiation, σ is the Stefan–Boltman constant, T_a is the air temperature, T_d is the dew point temperature, T_s is the temperature at the water surface, which is set to the water temperature in this study, f(wind) is a function of wind speed, and μ is a parameter related to the air temperature.

2.1.3 | Schemes for human water regulation

First, we coupled a widely used global reservoir regulation developed by Hanasaki, Kanae, and Oki (2006) into the RTM to control water and DIN. Based on the reservoir information (e.g., start year, main purpose, and storage capacity), the operation scheme set the operating rules for individual reservoirs. If a reservoir's primary purpose was not as an irrigation water supply, the reservoir operating rule was set to minimize interannual and sub-annual streamflow variation. If a reservoir was used as a primarily irrigation water supply, the released water from the reservoir was proportional to the water demand. Second, we considered the use of surface water (river water only) in the model. According to the irrigation water requirements, surface water was extracted from reservoirs or river channels. The specific equation can be written as follows:

$$S' = S - q_s\Delta t, \quad (9)$$

where Δt is the time step of CLM4.5, S and S' denote the surface water storage before and after withdrawing water, respectively, and q_s is the rate of surface water use. Finally, according to water consumption data, the extracted water is divided and added into some variables in the model for different purposes:

$$q_{top} = q_{top} + q_{irrg,sw}, \quad (10)$$

$$q_{evap} = q_{evap} + 0.7q_{ind,sw} + 0.7q_{dom,sw}, \quad (11)$$

$$q_{surf} = q_{surf} + 0.3q_{ind,sw} + 0.3q_{dom,sw}, \quad (12)$$

where q_{top} is the net water flow rate in the top soil layer, $q_{irrg,sw}$ is the irrigation water taken from the rivers, q_{evap} is the evaporation, q_{surf} is the surface runoff, and $q_{ind,sw}$ and $q_{dom,sw}$ are the water use for industrial manufacture and domestic consumption, respectively. The net water flow rate in the top soil layer is calculated based on the natural net water flux from precipitation and the anthropogenic water input rate from the water-use data mentioned in Section 2.2.2. In this work, we assumed that irrigation water was directly put into the soil surface, and the fractional non-irrigation water was regarded as evaporation and surface runoff after being used. According to a previous investigation (Zou, Xie, Yu, Zhan, & Sun, 2014), the coefficients in Equations 11 and 12 were temporally set to 0.7 and 0.3 due to the limitation of data.

A scheme of groundwater regulation was incorporated into CLM4.5 as a sub-model (Zeng et al., 2016; Zou et al., 2015). Groundwater pumping can be conceptualized as a process that extracts water from an aquifer. The groundwater withdrawal is written as follows:

$$W' = W - q_g\Delta t, \quad (13)$$

where W and W' are, respectively, the water storage in an aquifer before and after groundwater pumping, and q_g is the rate of groundwater exploitation. After groundwater pumping, the groundwater table changes as follows:

$$h' = h - \frac{q_g \times \Delta t}{s}, \quad (14)$$

where h and h' are, respectively, the simulated groundwater level before and after groundwater pumping, and s is the specific yield of the aquifer as determined by CLM4.5. It should be noted that W and h in this module considered the impact of water use by hydrological processes in soil, such as water infiltration. Finally, the extracted water was used for irrigation, industrial manufacturing, and

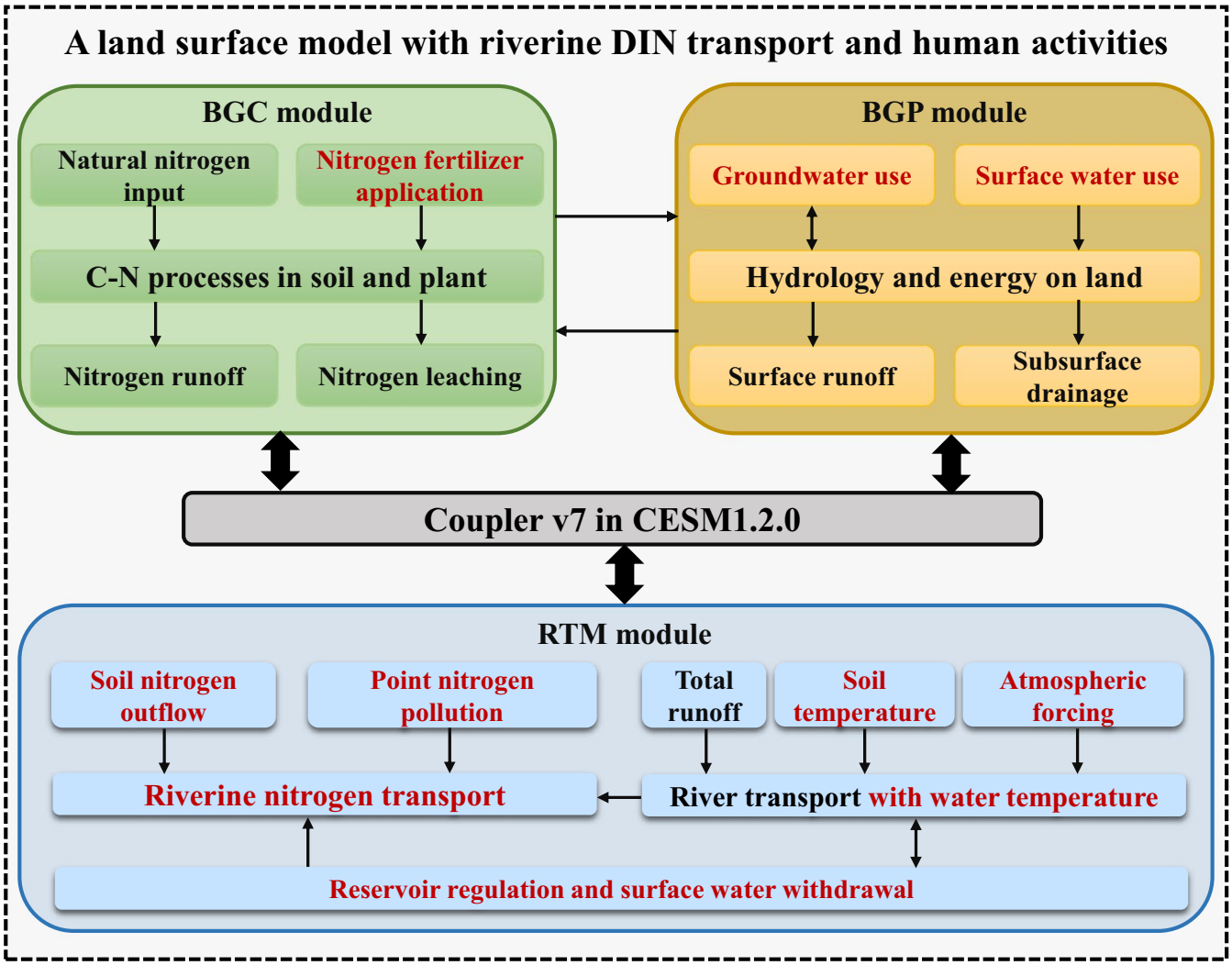

FIGURE 1 Schematic diagram of the land surface model with riverine nitrogen transport, anthropogenic nitrogen discharge and water regulation. The content with the black font are the original parts of the CLM4.5, while those with the red font are the newly added or modified parts presented in this work. In the global biogeochemical cycle (BGC) module, the nitrogen fertilizer data were replaced with a new dataset, while in the biogeophysical (BGP) module, we added schemes related to surface water use, and groundwater pumping and use. In the River Transport Model (RTM) module, we used the soil temperature and atmospheric data to calculate the river temperatures, and then implemented the riverine nitrogen transport with the disturbances from point-source pollution and surface water regulations. All the information exchange between either two modules was based on the coupler version 7 of Community Earth System Model (CESM1.2.0) model

domestic consumption, which was calculated as the same as that for surface water withdrawal.

2.1.4 | DIN transfer induced by water withdrawal and use

With the surface water regulation, the DIN in a given river grid cell changes. In this work, the riverine DIN was intercepted and released by reservoirs following the current riverine DIN concentration level. The extracted DIN values of surface water from the river systems were put back into cropland for BGC computing in the next time step. The deduction of DIN in the river flow is expressed as follows:

$$F_{N,out} = F_{N,out} - q_s \mathrm{con} \Delta t, \quad (15)$$

Meanwhile, we suppose that the amount of extracted DIN, which is put back into the soil top layer for BGC computing, is calculated based on the mean DIN concentration in the soil and the amount of pumped groundwater. The deduction of DIN in groundwater is written as follows:

$$\mathrm{Leaching}_N = \mathrm{Leaching}_N - q_w \mathrm{scon} \Delta t, \quad (16)$$

where scon is the mean DIN concentration in the soil. Finally, the extracted DIN from both surface water and groundwater is put back into the land, which is expressed as follows:

$$\mathrm{Fer} = \mathrm{Fer} + (1 - \mathrm{Frac}) q_s \mathrm{con} \Delta t + q_g \mathrm{scon} \Delta t, \quad (17)$$

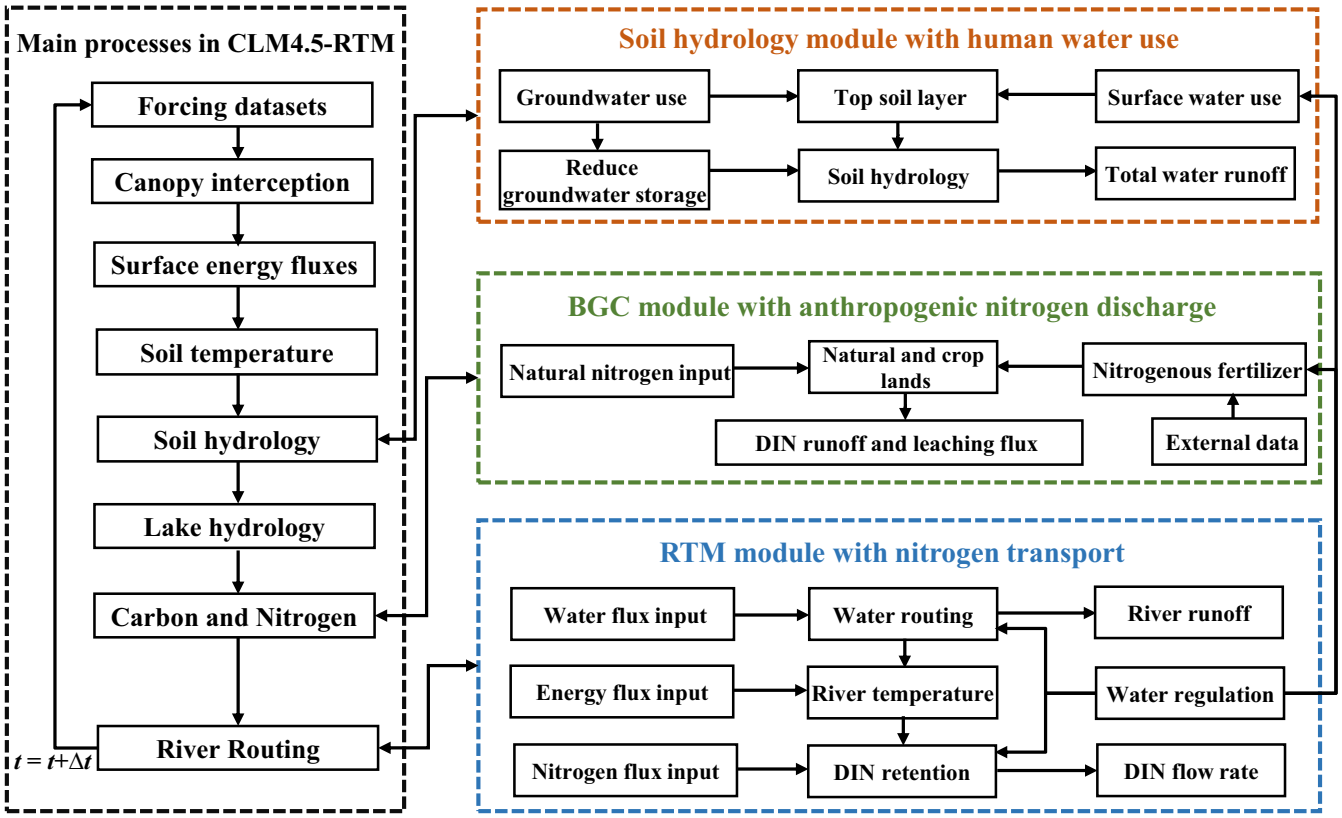

FIGURE 2 Main calculation process in CLM4.5-RTM and its coupling with riverine nitrogen transport and anthropogenic activities. The content in the black dashed box displays the main calculation process in CLM4.5-RTM, while the details in the orange dashed box show how the schemes of human water use were coupled with the soil hydrology module. The information in the green dashed box show how external nitrogen data was used in the BGC module, while the blue dashed box shows how the schemes of nitrogen transport and river temperature were implemented within the RTM module. BGC: global biogeochemical cycle; CLM: Community Land Model; RTM: River Transport Model

where Fer indicates the nitrogen input rate into the soil. Frac used here suggests that the assumptive amount of DIN loss during the water diversion is determined by the proportion of DIN retention in the rivers. Because groundwater pumping and usage usually occur in the same region, we suppose there is little amount of DIN loss by groundwater exploitation.

2.1.5 | Integrated modeling framework

In this work, a land surface model with riverine nitrogen transport and water regulation was established based on the integrated modelling framework of CESM1.2.0, in which the land surface model contained a BGP module, a BGC module, and a RTM, as shown in Figure 1. The BGP module was used for water and energy calculations, such as runoff, evapotranspiration, soil temperature, and vertical heat flow rate, while the BGC module was used for ecological processes calculations, such as the leaf area index (LAI), the stem area index (SAI) and carbon-nitrogen pools. The RTM was used for river routing. When the BGC module is activated, the coupled interaction between the BGP and BGC modules begins. The BGP module provided some variables, such as runoff, soil water, soil temperature, for the calculation of carbon and nitrogen allocation in plants and soil, decomposition, nitrogen runoff, and leaching in the BGC module. Next, the BGC module returned some variables, such as the LAIs and/or SAIs, which affected the BGP module computation. The original RTM was almost an offline diagnostic module, which obtained runoff information from the BGP module by the coupler in CESM1.2.0. If the RTM runs at a finer resolution than the CLM, the CLM runoff will be automatically interpolated to the RTM grid by the coupler. Hence, we incorporated the schemes of the riverine nitrogen transport and human water regulation into this coupled modeling framework as follows:

1. Based on the original RTM and the model coupler, we built and integrated a large-scale scheme of riverine nitrogen transport into it, using Equations 2–6. This module received the water runoff from the BGP module, the soil nitrogen losses from the BGC module, and point source nitrogen pollution from external datasets. Meanwhile, we used the coupler to transfer the soil water temperature, solar radiation, relative humidity, and wind speed to the RTM module for the large-scale river temperature modelling, using Equations 7 and 8. Furthermore, we coupled global reservoir regulation into the RTM to regulate water and DIN. Then, surface water withdrawal and corresponding DIN were calculated using Equations 9 and 15. Finally, the extracted water and DIN from the river system

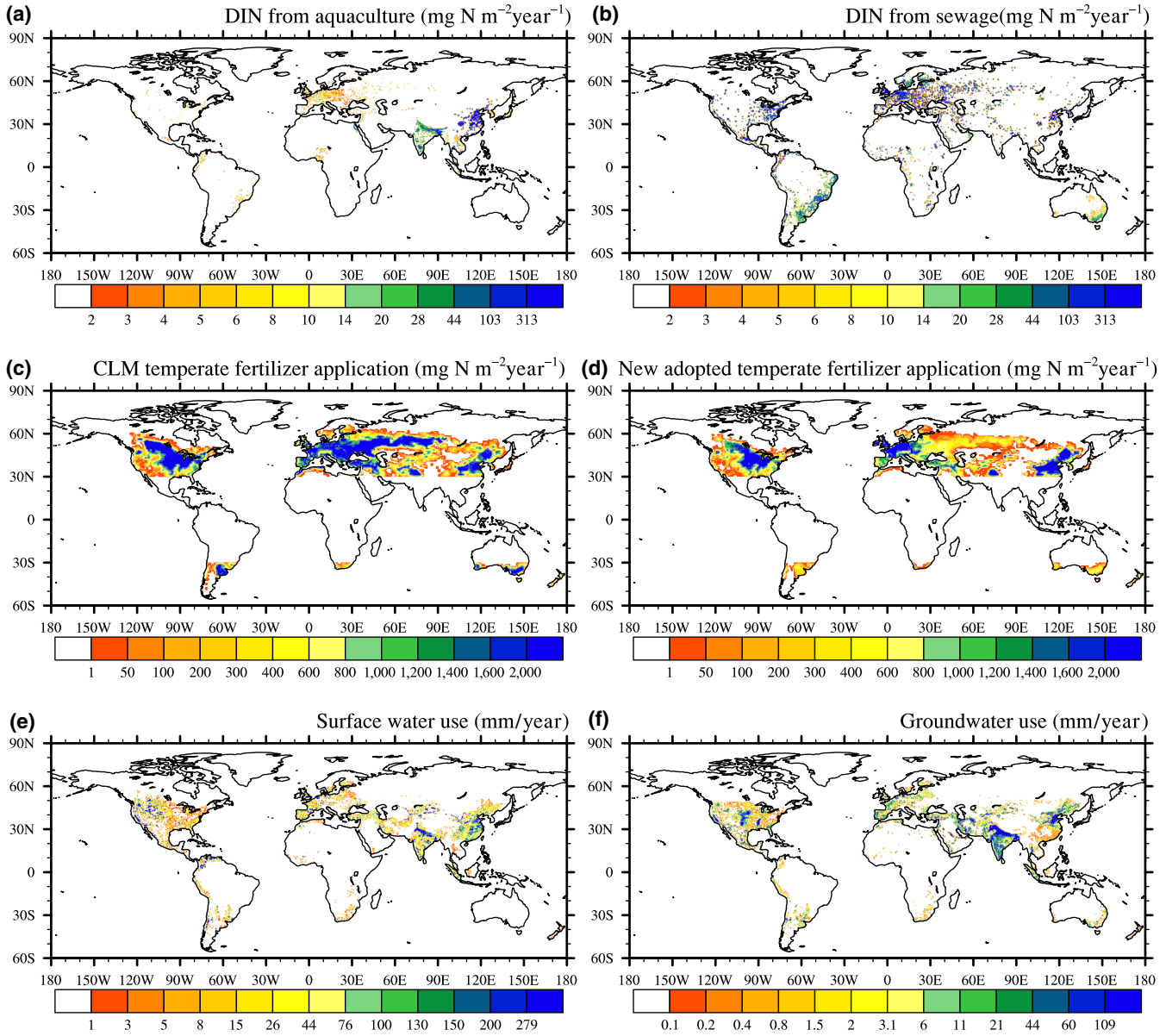

FIGURE 3 Spatial distributions of the multi-year averaged data on the human activities including (a) discharged DIN from aquaculture, (b) discharged DIN from sewage, (c) default temperate fertilizer data in CLM4.5, (d) the newly adopted temperate fertilizer data, (e) surface water usage amount, and (f) groundwater usage amount. CLM: Community Land Model; DIN: dissolved inorganic nitrogen

were put back into the BGP and BGC modules via the model coupler. Although the last step may cause more uncertainties, it can express a more real process, at least.

2. In the BGP module, we added schemes related to groundwater pumping using Equations 13 and 14. We suppose that the amount of extracted DIN is calculated using Equation 16. Then, the water used for irrigation, industrial manufacturing, and domestic consumption were also considered using Equations 10–12. These newly added water usages could absolutely change the water and heat flow rates to plants and the soil, and the BGC processes.
3. In the BGC module, the original fertilizer amount was fixed for each temperate crop, which may not properly reflect reality in the global simulation. Therefore, we used a new gridded nitrogen fertilizer dataset, which were based on statistical materials, to replace the default data. As well, this module can receive the extracted DIN from both the surface and underground water withdrawal, using Equation 17.

Figure 2 shows the main calculation process in the modified CLM4.5-RTM. We can see that although all the processes happen simultaneously, the computation order in the man-made model is mainly surface water and energy interception, surface energy flux, hydrological and ecological calculations in vegetation and soil, and river routing in the original CLM4.5-RTM. In this work, based on this sequence, each new integrated part runs when the corresponding master module is activated. When the soil hydrology module begins calculating, the data on groundwater use will be read in, and the code for human water use, including irrigation and groundwater

TABLE 1 Main data for model running and validation

Main data	Resolution	Time	Source
CRUNCEP forcing	0.5°/6 hr	1901–2010	Piao et al. (2012)
Land cover	0.05°/3 hr	Constant	IGBP soil dataset
Soil dataset	1 km	Constant	
Elevation	1 km	Constant	USGS HYDRO1K dataset
Flow direction	0.5°	Constant	Oleson et al. (2013)
Nitrogen fertilizer	0.5°	1961–2013	Lu and Tian (2017)
Municipal wastewater	0.5°	1960–2013	Morée et al. (2013)
Aquacultural pollution	0.5°	1960–2013	Bouwman et al. (2013)
Water use	Country	1958–2017	FAO
Map of irrigation areas	0.5°	Constant	Siebert et al. (2013)
Map of irrigation intensity	0.5°	Constant	Zeng et al. (2017)
DIN concentration	Site	Values around 1995	Drecht et al. (2003); Seitzinger et al. (2005)
River temperature	Site	Mean monthly value around 1990	Beek et al. (2012); Van Vliet et al. (2011); Van Vliet et al. (2012); Van Vliet et al. (2013)

DIN: dissolved inorganic nitrogen.

pumping, will be executed. When the BGC computation starts, the external data on nitrogen fertilizer will be read in, and these data will be added to the croplands, namely the crop column defined in the sub-grid structure of CLM4.5. After all the vertical computations in each grid cell of CLM4.5 are completed, the total water runoff and DIN runoff and leaching are prepared for river water routing and nitrogen transport. When the RTM begins, the external data on point source pollution, surface water use and reservoir are read in. Then, the water, energy and DIN are transported by the river system and regulated by anthropogenic surface water utilization. The extracted surface water and DIN is deducted in the current river system at this time step and then they are put back to the corresponding grid cell in CLM4.5 by the model coupler for the soil hydrological and ecological calculations in the next time step. Finally, the modified CLM4.5-RTM provides us with the river water temperature, DIN flow rate and some different results of CLM4.5 with considered human activities.

2.2 | Basic data

2.2.1 | Atmospheric and land surface data

The CRUNCEP is a 110-year (1901–2010) dataset that provides standard forcing for CLM4.5 (Piao et al., 2012; Viovy, 2011). It is a combination of two existing data sets: the CRUTS 3.2 0.5° × 0.5° monthly data that covers the period 1901–2002 (Mitchell & Jones, 2005) and the NCEP reanalysis 2.5° × 2.5° 6-hourly data that covers the period 1948–2010. CLM4.5 was equipped with the comprehensive surface dataset described in the technical notes (Oleson et al., 2013). The surface data included the land cover type from MODIS satellite data, soil textures from the International Geosphere-Biosphere Programme soil dataset, and the elevations from the USGS HYDRO1K dataset. The river system used the standard RTM flow direction dataset at 0.5° × 0.5° spatial resolution.

2.2.2 | Human activity data

Based on the statistical data from the IFA (International Fertilizer Industry Association) and FAO (Food and Agricultural Organization) surveys of country-level fertilizer input, Lu and Tian (2017) developed a global time series data of annual synthetic nitrogen fertilizer usage rates in agricultural lands, which were matched with the HYDE 3.2 historical land usage maps, which had a resolution of 0.5°, from 1961–2013. In this work, we extracted the data for temperate croplands in CLM4.5, and reshaped the data to a new spatial resolution of 1°. More precisely, first we extracted the original fertilizer data map across the temperate croplands defined in CLM4.5 with a resolution of 0.5°. Then, the mean fertilizer application rate across the croplands in each grid cell was converted to the averaged value across all grid cells. After this, bilinear interpolation was used to reshape the data to a new spatial resolution of 1°. Finally, we obtained the fertilizer application rate over the croplands in each 1° grid cell.

Point sources of DIN are primarily associated with municipal and aquacultural wastewater. The dataset on DIN discharge from municipal wastewater was from the work of Morée, Beusen, Bouwman, and Willems (2013), while the aquacultural DIN pollution data was from the work of Bouwman et al. (2013). In the current work, these two kinds of DIN inputs were merged to form the one-point sources of pollution, which were assumed to directly discharge into the river systems. The multi-year averaged data are shown in Figure 3. We can see that the point sources of pollution were mainly distributed in the eastern USA, western Eurasia, southern regions of South America, India, and China. It is seen that the middle of the USA,

TABLE 2 Experimental design in this work

Group	Resolution	Period	Default fertilizer data	New fertilizer data	Point source pollution	Human water regulation
EXP1	1°/0.5°	1991–2010	✗	✗	✗	✓
EXP2	1°/0.5°	1991–2010	✗	✓	✗	✓
EXP3	1°/0.5°	1991–2010	✗	✓	✓	✓
EXP4	1°/0.5°	1991–2000	✓	✗	✓	✓
EXP5	1°/0.5°	1991–2000	✗	✗	✗	✗

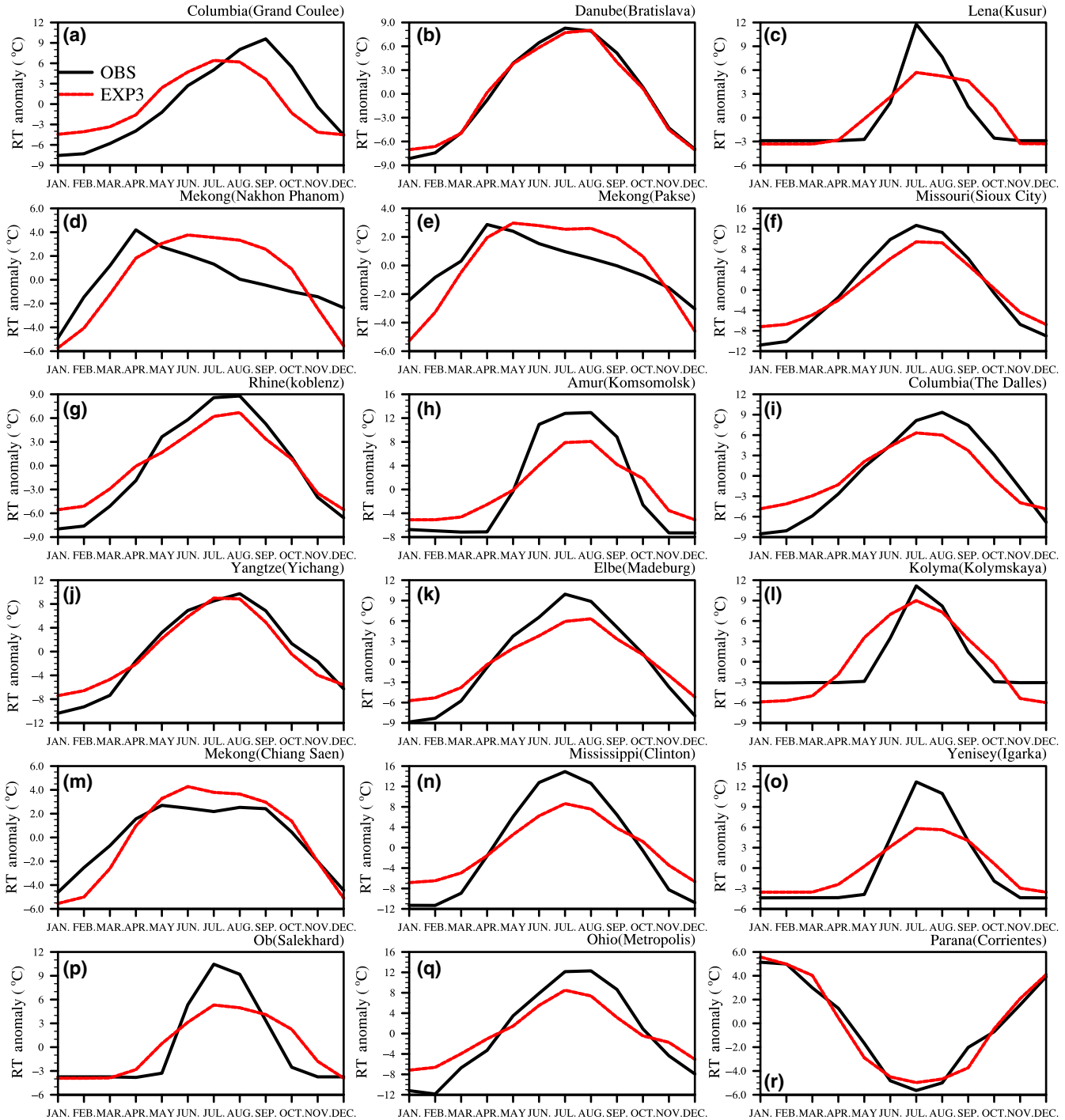

FIGURE 4 Comparisons between observed and simulated monthly river temperatures (RT) anomaly from EXP3 at 18 gauged stations

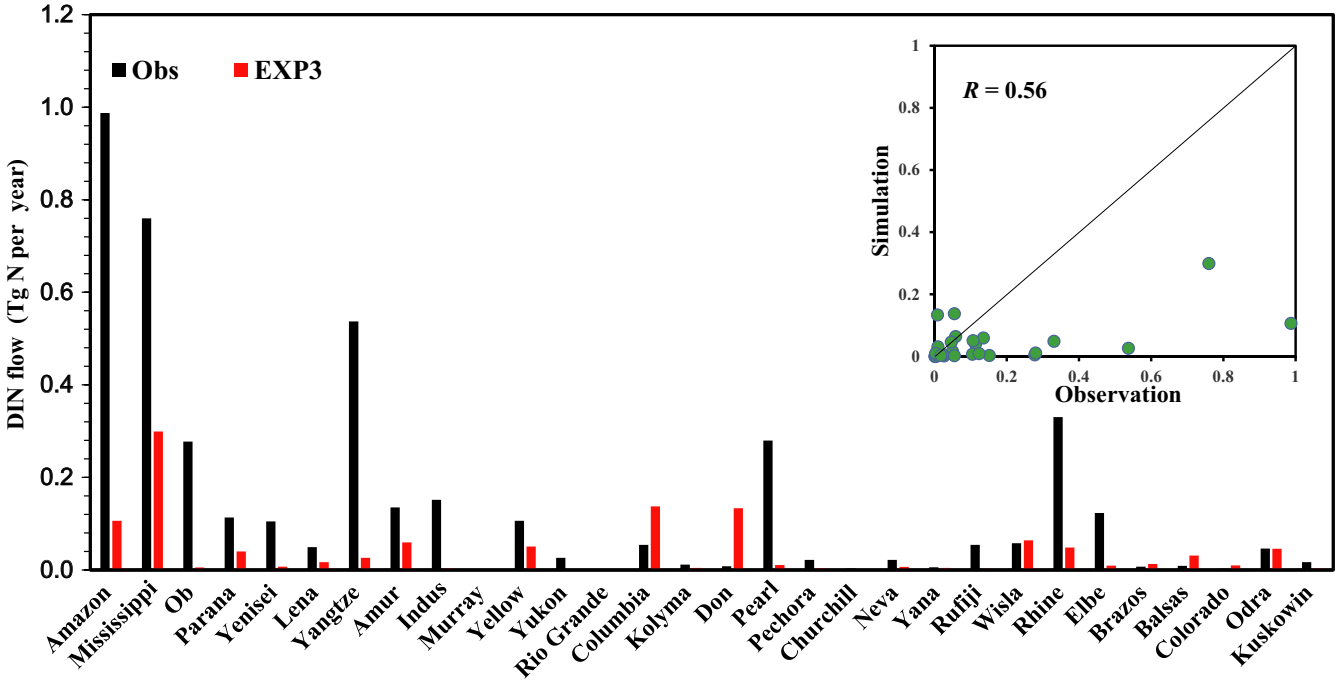

FIGURE 5 Bar chart and scatter plot of the simulated and observed riverine DIN flow rates at 30 large river mouths over the world. The black bars are observations from literature records, while the red bars are the simulated results from EXP3

western Eurasia and the northeast of China used the largest amount of nitrogen fertilizer. From Figure 3c–d, we also could see that the newly adopted fertilizer data had a better spatial heterogeneity than the default one within CLM4.5.

A dataset of power stations dumping heat into rivers was taken from the dataset available in Raptis and Pfister (2016), excluding emissions into lakes. A total of 1,750 generating units were selected, pertaining to 565 power stations, which account for 12% of the global thermoelectric power capacity. The majority of power plants with once-through cooling systems are identified in the Northern Hemisphere and along major rivers.

Before considering the effects of human water use in the model, the necessary long-term global gridded data of water usage needed to be estimated. For this purpose, we collected five datasets. The first data source was from the FAO water use dataset (http://www.fao.org/nr/water/aquastat/data/query/index.html), which provided us with the annual surface water and groundwater consumption of about 200 countries across the world from 1958 to 2017. The second was a shape file data of world map including 265 national boundaries. The third dataset was the Global Map of Irrigation Areas, version 5.0 (Siebert, Henrich, Frenken, & Burke, 2013), which showed the size of areas equipped for irrigation, and the size of each area that was irrigated using surface water and groundwater in each grid cell. The fourth data source consisted of historical monthly soil moisture levels and saturated soil moisture levels simulated by CLM4.5 offline for the years 1965–2000 (Zeng et al., 2017), which was used to determine a map of irrigation intensity. The fifth dataset was from the FAO water information system for 2010, which contained regional water withdrawal data and expressed the agricultural, industrial, and municipal water withdrawals as percentages of the total global withdrawal (http://www.fao.org/nr/water/aquastat/main/index.stm).

First, based on the first and the second datasets, we determined the long-term and spatially distributed annual amount of surface water and groundwater uses, respectively, at the country level for the whole world. Then we used the second, third, fourth, and fifth datasets to estimate the spatial allocation proportions of surface water and groundwater demands in each country for agricultural, industrial, and domestic water uses. Using these reprocessed data, we downscaled the annual data from the country level to the grid cell level. Then, in order to make the data change seasonally, we empirically set some user-defined monthly allocation proportions of agricultural water use for different latitude zones to further downscale the temporal resolution of some data from yearly resolution to monthly resolution. Finally, a long-term and spatially explicit water use dataset from 1958 to 2017 was estimated for the numerical modeling. From Figure 3e,f, we can see that surface water was widely used, and groundwater was frequently used only in the middle of the USA, the north of India and northern China.

2.2.3 | Observational data

In this study, lateral DIN flows were included so that the chemical flow rates at the global scale could be validated using actual measurements from river outlets. For the preliminary validation of the modelled riverine nitrogen transport, we collected the observed DIN concentrations from 30 large rivers across the world from literature records, which were the published values from around 1995 (Drecht, Bouwman, Knoop, Beusen, & Meinardi, 2003; Seitzinger et al., 2005). In addition, we obtained the river temperature data series from

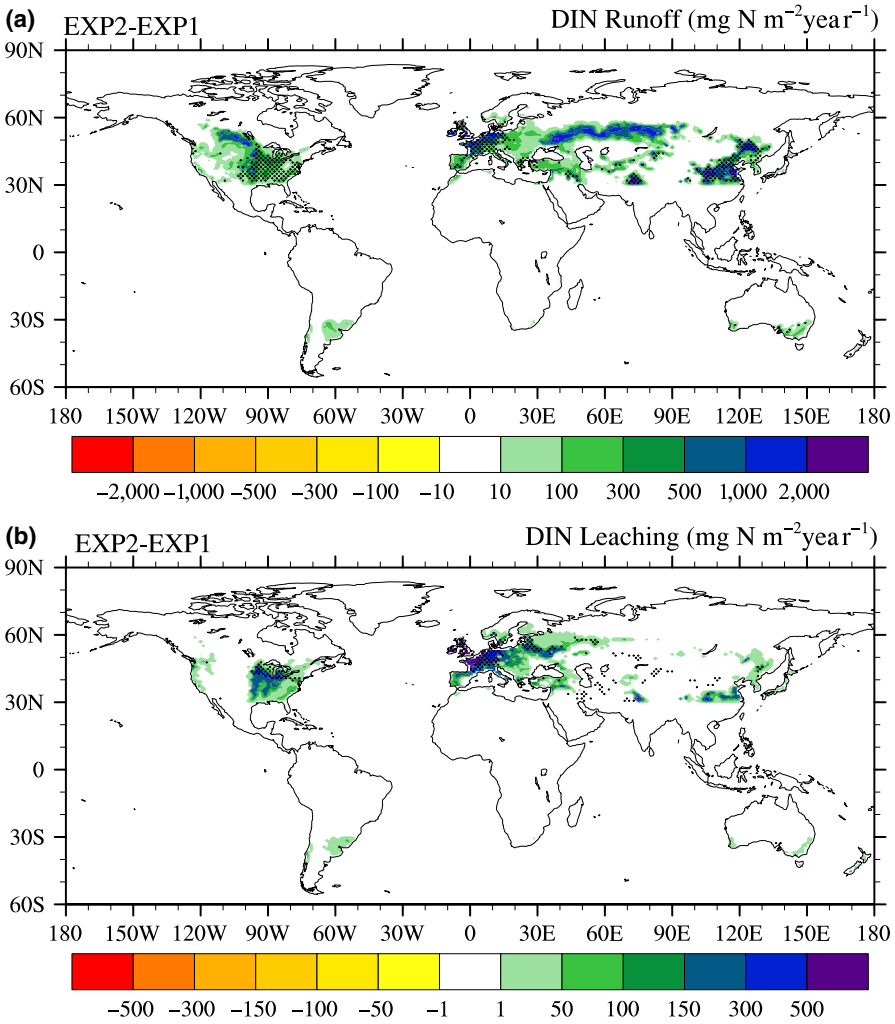

FIGURE 6 20-year averaged spatial distributions of the differences between EXP2 and EXP1 in: (a) soil dissolved inorganic nitrogen (DIN) runoff and (b) soil DIN leaching. This figure reflects the effects of temperate fertilizer application on the DIN losses from soil. The black dots indicate regions where the difference passed the 95% confidence level of the Student's *t* test

previous related work (Beek, Eikelboom, Vliet, & Bierkens, 2012; Van Vlietet al., 2013, 2012; Van Vliet, Ludwig, Zwolsman, Weedon, & Kabat, 2011). Most data originated from the GEMS/Water (http://www.gemswater.org/) monthly climatology data. We used the widespread observations around 1990 at 18 sites to validate the water temperature simulation. Table 1 lists the main data used in the study.

2.2.4 | Experimental design

Using the basic datasets described above, three main simulations were conducted using the developed model, as shown in Table 2. All simulations were conducted with the fully prognostic carbon and nitrogen cycle modules accompanied by the crop module. The first simulation (EXP1) was run without fertilizer usage and point source pollution, which was considered as the baseline experiment. The second simulation (EXP2) included fertilizer usage. The last simulation (EXP3) considered both fertilizer usage and point source pollution. Due to the limitation of available computing resources, the spatial resolution of the model was fixed to about 1° for land, and 0.5° for river transportation. The time step was 1800 s for land processes, and 3 hr for river systems. First, we ran the original land surface model without human activities for about 1,000 years to reach an equilibrium state. Then, using these results as the initial state, we ran the simulation from 1986 to 2010. The first 5 years (1986–1990) was used as the spin-up period for the river systems, while the output from the last 20 years (1991–2010) were used for result analyses.

Some sensitivity tests were added, as shown in Table 2. The first case was an investigation of the impact of different fertilizer data on soil nitrogen runoff and leaching, both of which, to a great extent, determined the amount of DIN in the rivers. For this case, there were two experiments: one that used the default data (EXP4), and the other that used the new fertilizer data (results from EXP3). The second case was devised to help us understand any uncertainties that arose from the water regulation modeling. Along these lines, we set a new experiment (EXP5), which did not activate nitrogen discharge or water use. These supplementary experiments were run for only 10 years, from 1991 to 2000. The initial conditions and other data forcing from 1991 were the same as the 20-year simulations from 1991 to 2010 mentioned above.

In addition, to show the importance of river temperature computing for riverine DIN transport modeling, we conducted two control tests consisting of DIN transport modeling with and without dynamic river temperatures. For these two tests, the simulation period was only 3 years with repeated forcing in 2000 and the initial condition is as same as other experiments.

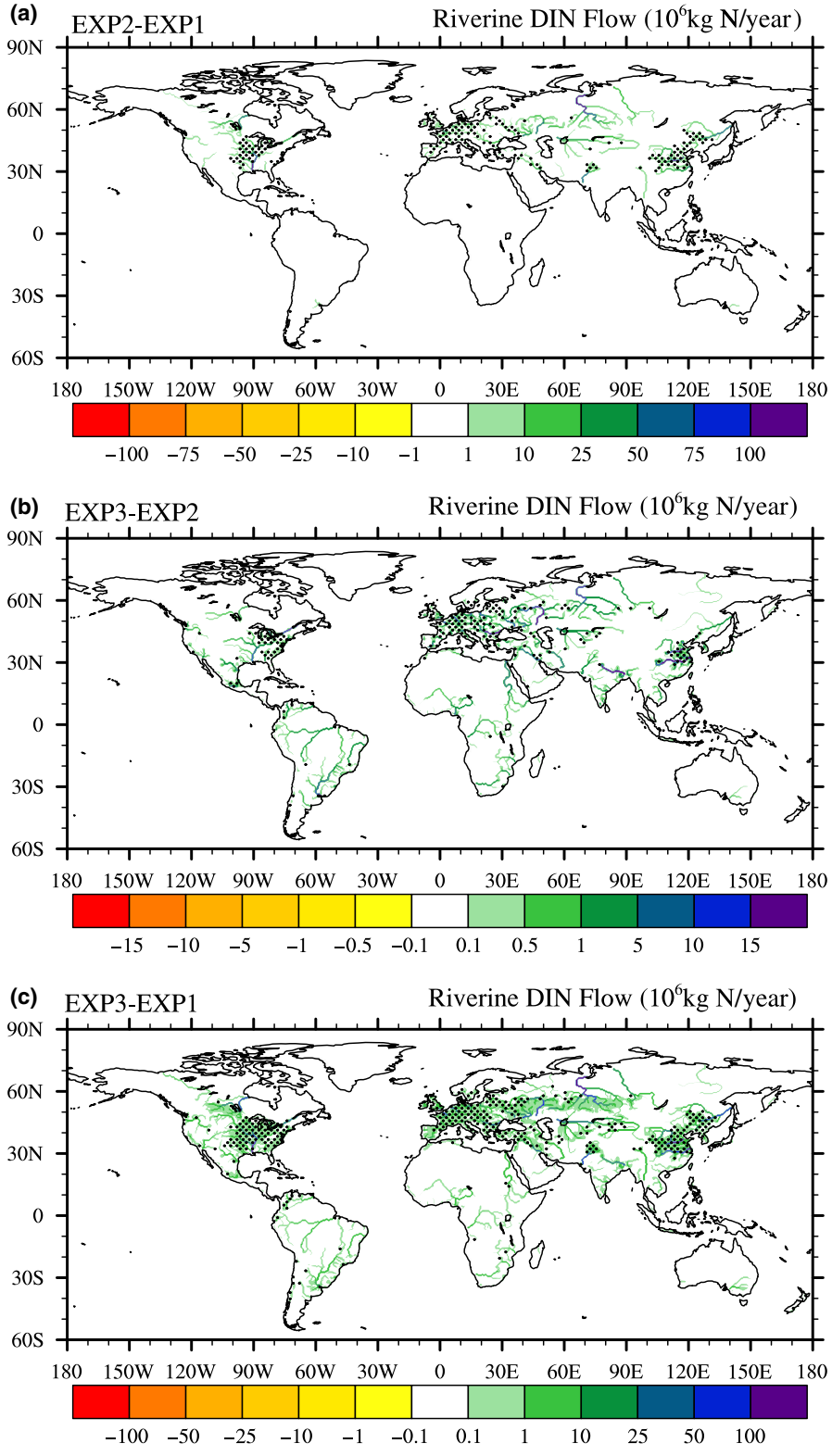

FIGURE 7 20-year averaged spatial distributions of the differences in the riverine DIN flow rates between different experiments: (a) EXP2 and EXP1, (b) EXP3 and EXP2, and (c) EXP3 and EXP1. This figure demonstrates the effects of temperate fertilizer application, point source pollution, and their combined effect on the anthropogenic nitrogen discharge on the riverine DIN flow rates. The black dots indicate regions where the difference passed the 95% confidence level of the Student's *t* test

3 | RESULTS

3.1 | Validation for river water temperature and DIN transport modeling

According to our previous studies (Xie et al., 2018; Zeng et al., 2017), we found that considering human water regulation could make the results of soil moisture, evaporation and river water flow more reasonable. In this work, we checked the reasonability of river water temperature and DIN flow rate modeling. Figure 4 shows a comparison of river temperature from observations and the simulation at 18 selected sites. It can be seen that at most sites the model can accurately capture the monthly change. The Pearson's

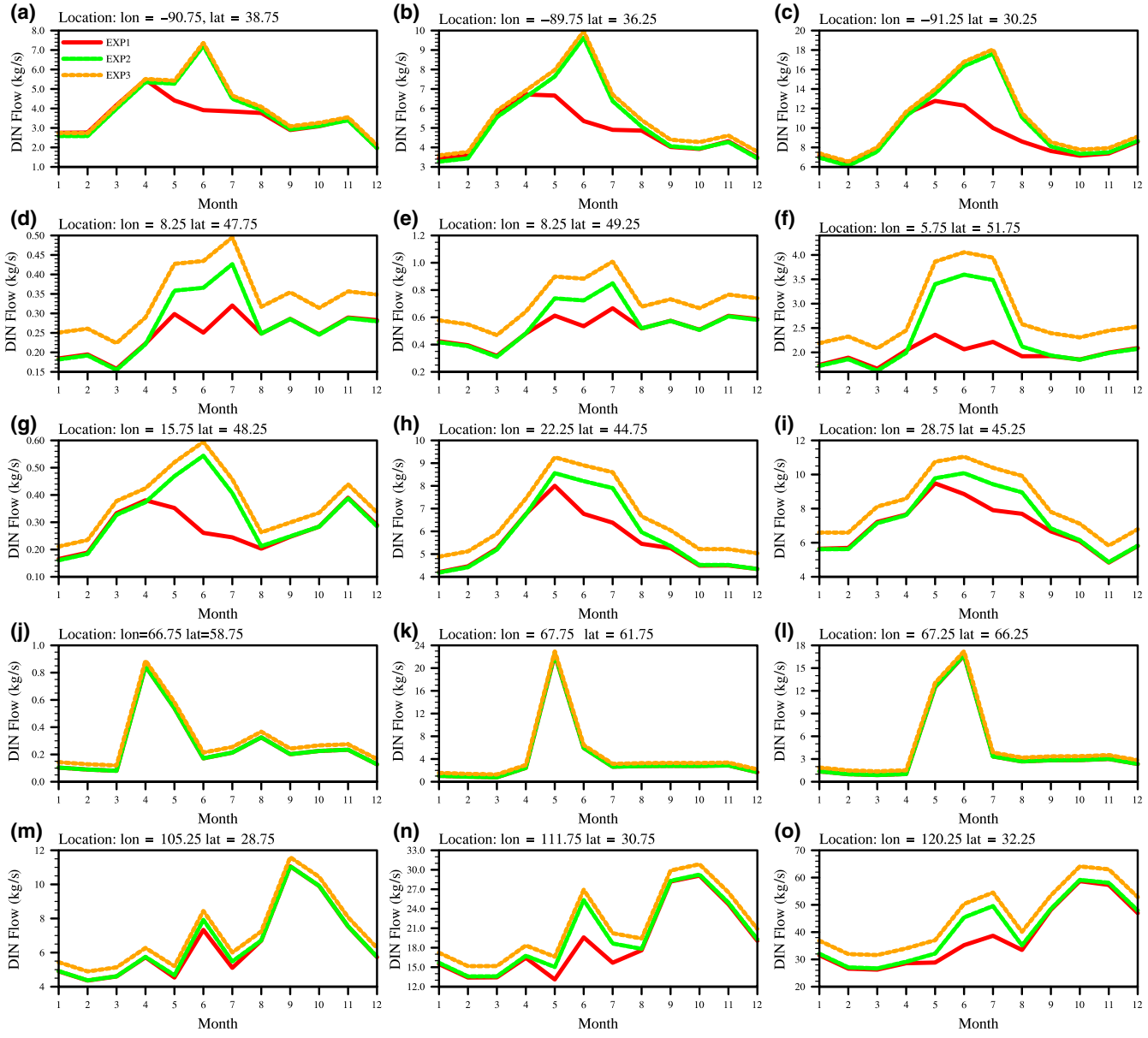

FIGURE 8 Time series of the mean monthly dissolved inorganic nitrogen (DIN) flow rates simulated by EXP1 (red line), EXP2 (green line) and EXP3 (orange line). The five rows from top to bottom, respectively, denote the Mississippi River in the USA, the Rhine and the Danube in Europe, the Ob River in Russia, and the Yangtze River in China. The three columns from left to right, respectively, represent three locations at the upstream, the middle reaches, and the downstream in each river. The longitude and latitude of each location are also shown on the top of each plot, and the unit is degrees

correlation coefficient averaged at the 18 sites was about 0.81, which indicates that the developed model has the ability to reproduce the changes in river temperature. Figure S1 in the supporting information presents the effects of water temperature modeling on the seasonal changes in DIN. The red line means the *rt* in Equation 6 is fixed to 20°C, while the green line indicates that the *rt* is calculated by Equations 7 and 8. The results show that the river temperature modeling makes the seasonal changes in DIN discharge smaller. If we do not consider dynamic water temperatures, the changes in DIN discharge are mainly controlled by the changes in the total amount of DIN runoff and leaching from the soil. On the contrary, when the amount of DIN into rivers with the help of more rainfall and used fertilizer increases in warm seasons, the higher river water temperature will result in more DIN in rivers being lost or converted to another chemical forms by the effects of denitrification, sedimentation, and uptake by aquatic plants, which is conceptually expressed in Equation 4. The changes in colder seasons abide by the similar principle.

Figure 5 shows a comparison between the observed DIN flow rates and the simulated ones from EXP3 at 30 large river mouths across the world in 1995. The *y*-axis is the annual DIN flow rate of an individual river mouth. The *x*-axis shows the river names, which are ordered in size from the largest to the smallest river basin. The results demonstrated that the developed model underestimated

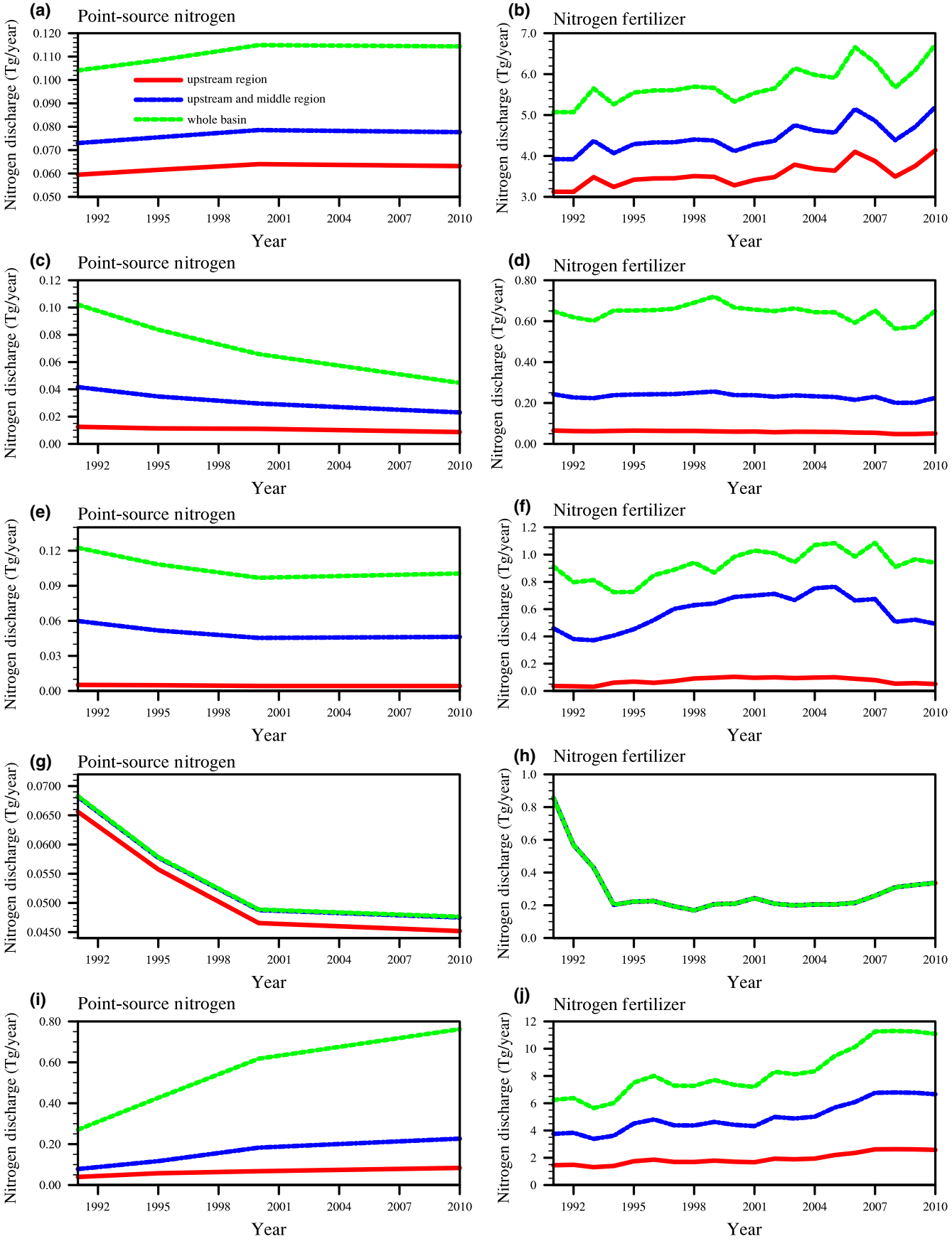
(a)
Point-source nitrogen
upstream region
upstream and middle region
whole basin
Nitrogen discharge (Tg/year)
Year
(b)
Nitrogen fertilizer
(c)
Point-source nitrogen
(d)
Nitrogen fertilizer
(e)
Point-source nitrogen
(f)
Nitrogen fertilizer
(g)
Point-source nitrogen
(h)
Nitrogen fertilizer
(i)
Point-source nitrogen
(j)
Nitrogen fertilizer

FIGURE 9 Time series of the annual anthropogenic nitrogen discharge that include fertilizer use and point source discharge. The five rows from top to bottom, respectively, denote the Mississippi River in the USA, the Rhine and the Danube in Europe, the Ob River in Russia, and the Yangtze River in China. The two columns from left to right, respectively, represent the amount of point source nitrogen pollution and fertilizer application in regions that are upstream of the selected locations in the river basins in Figure S2. The red, blue, and green lines represent the catchments upstream of the selected locations, respectively, in the upstream, middle reaches, and downstream of each river

the riverine DIN flow rates at most selected sites. However, the simulated results have the same order of magnitude as the observations. The correlation coefficient was 0.56. Consequently, we considered that the model reproduced the DIN flow rates for selected rivers with a reasonable accuracy for the global large-scale modeling.

3.2 | Effects of anthropogenic nitrogen discharge on the riverine DIN

Figure 6 shows multi-year averaged spatial patterns of the differences in the DIN runoff and leaching in the soil between EXP2 and EXP1. It can be clearly seen that the nitrogen fertilizer discharge directly

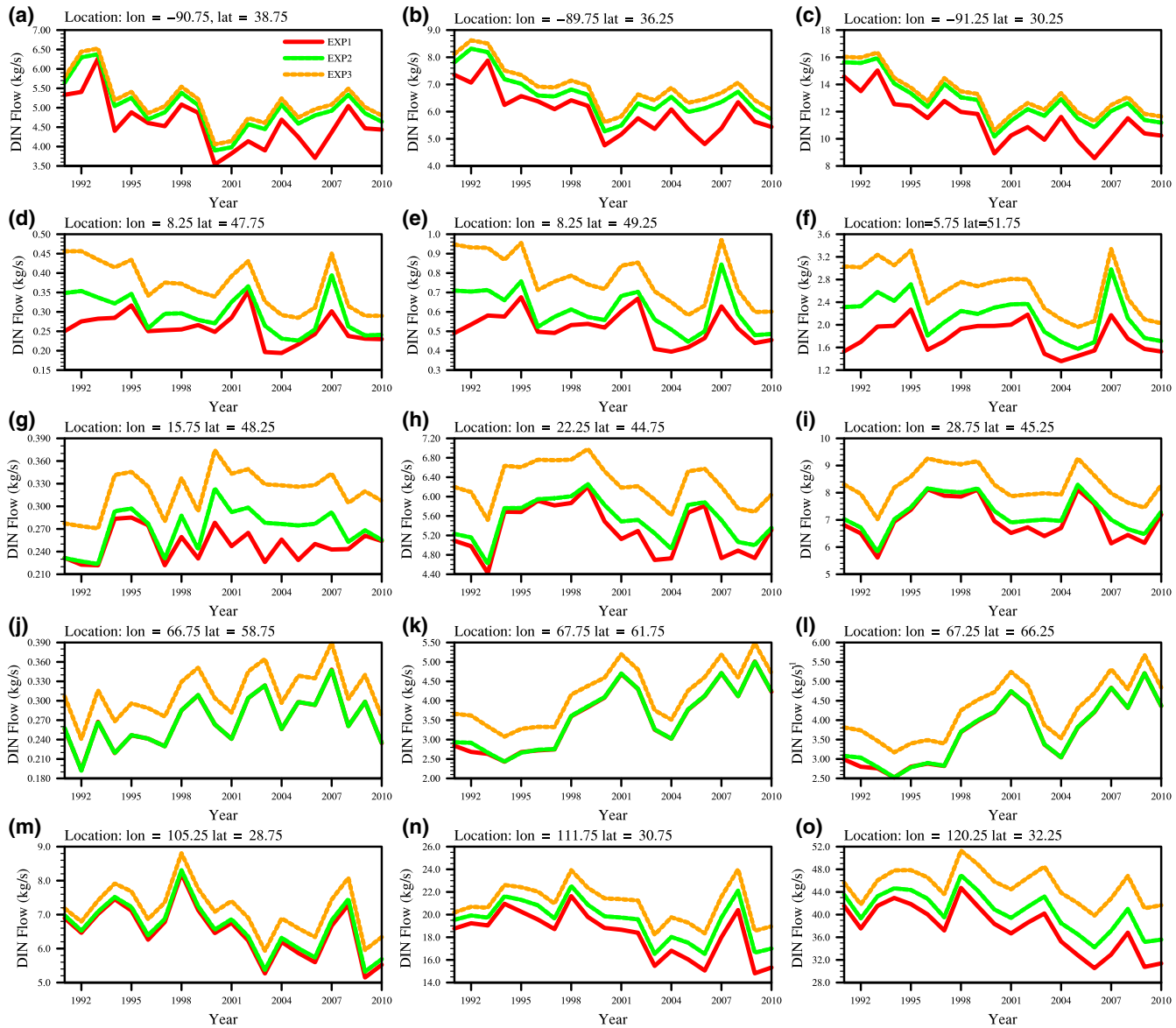

FIGURE 10 Time series of the mean annual dissolved inorganic nitrogen (DIN) flow rates simulated by EXP1 (red line), EXP2 (green line) and EXP3 (orange line). The five rows from top to bottom, respectively, denote the Mississippi River in the USA, the Rhine and the Danube in Europe, the Ob River in Russia, and the Yangtze River in China. The three columns from left to right, respectively, represent three locations at the upstream, the middle reaches, and the downstream in each river. The longitude and latitude of each location are shown on the top of each plot, and the unit is degrees

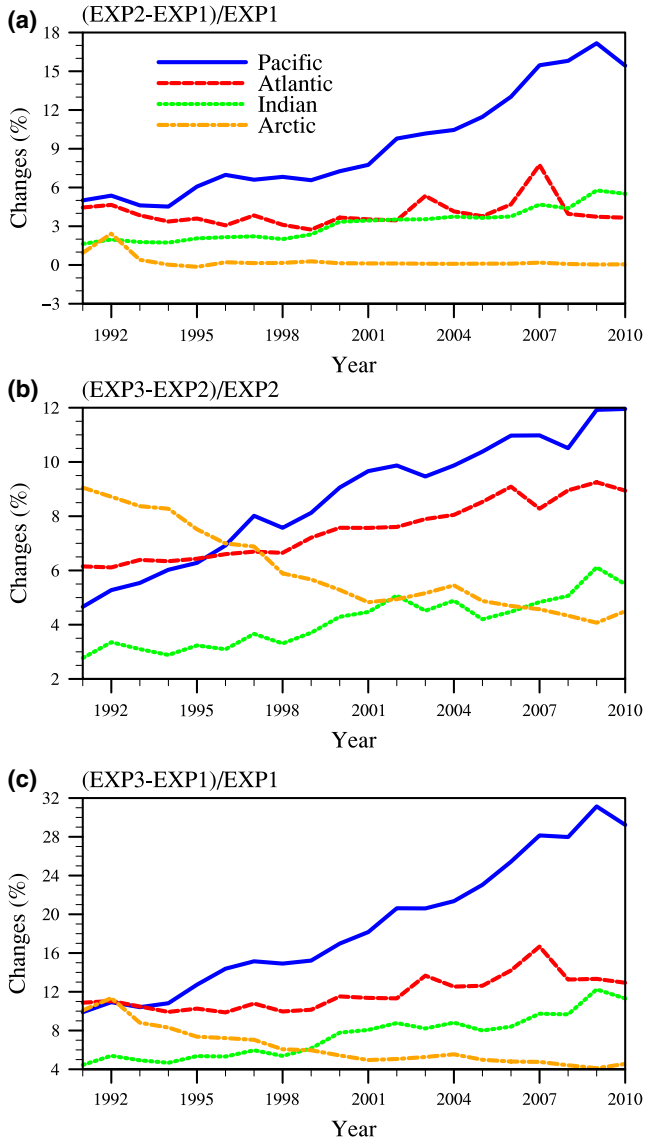

FIGURE 11 The 20-year time variation of the impact of anthropogenic nitrogen discharge on the riverine dissolved inorganic nitrogen (DIN) exported to oceans. This figure demonstrates the effects of (a) temperate fertilizer application, (b) point source pollution and (c) the combined effect of these sources of anthropogenic nitrogen discharge on the exported DIN

increased the soil DIN losses from both surface runoff and subsurface leaching. From the aspect of DIN runoff, temperate fertilizer application caused the DIN runoff to increase most significantly in the eastern USA, western Europe, and in the north and northeast of China. Most increments occurred in Germany, France, England, Iran, Russia, and China. The largest increases were about 2,000 mg m^{-2} $year^{-1}$. From the aspect of DIN leaching, the effects of fertilizer application were different in the spatial distribution. We could see that only the middle and east of the USA and the western Europe were largely affected, where the largest increases were about 500 mg m^{-2} $year^{-1}$, which was lower than that of the modeled DIN runoff.

Figure 7 displays the multi-year averaged spatial patterns of the effects of temperate fertilizer application and point source pollution on the riverine DIN flow rates across the world. Figure 7a demonstrates that nitrogen fertilizer application increased the DIN in the rivers, especially in the middle of the USA (the Mississippi River), western Europe, and the north of China (the Yellow River and the Yangtze River). The annual flow rates in most affected rivers increased by 20,000–40,000 tons. Figure 7b shows the contributions of point source nitrogen pollution to the riverine DIN flow rates. We can see that almost all the large rivers in the world have been affected by widespread human activities. The rivers in western Europe and eastern China were the most polluted, where the annual DIN had increased by 5,000–15,000 tons. Figure 7c shows the combined effects of temperate fertilizer application and point source nitrogen pollution, which reflects the notion that anthropogenic nitrogen discharge could directly and markedly augment the amounts of DIN in most rivers across the world, and is hence an important factor related to riverine environmental problems. Undoubtedly, the Mississippi River Basin, the Yellow River Basin, the Yangtze River Basin, and western Europe are the most polluted regions.

We took five large rivers as case studies to show how human nitrogen input can influence the mean monthly and annual DIN flow rate in rivers. The selected rivers were the Mississippi River in the USA, the Rhine and the Danube in Europe, the Ob River in Russia, and the Yangtze River in China, as shown in Figure S2. Then, we empirically chose three sites located at the upstream, the middle, and the downstream of each river. Figure 8 shows the mean monthly DIN flow rates simulated in EXP1 (red line), EXP2 (green line) and EXP3 (orange line). The five rows denote the five rivers, and the three columns represent the three locations. It can be seen that nitrogen fertilizer application obviously influenced the Mississippi River, the Rhine, the Danube, and the Yangtze River, while the Ob River was hardly affected. During the fertilization period, all the DIN flow rates at the different locations increased. In most rivers, the effect of fertilizer use became bigger and bigger from the upstream to the downstream river, which reflected the characteristic of riverine nutrient enrichment. The Yangtze River and the Mississippi River were affected by fertilizer application more seriously compared to the others. However, it should be noted that only temperate fertilization was considered in the current version of the land surface model, so that the effects on the Yangtze River may be underestimated because almost half of the river basin belongs to a subtropical zone. More uncertainties about the shortcomings of the model were discussed in the following sections. From the perspective of point source nitrogen pollution, we can see that the pollution only mildly affected the mean monthly DIN flow rates in both the Mississippi River and the Ob River. The Yangtze River was the most polluted, while the aquatic environments in the Rhine and the Danube were also threatened. Because the original pollution data were for each year, the effects showed nearly the same bias for each month in a single year.

Figure 9 shows the annual changes in the nitrogen discharge into soil and rivers by fertilizer application and point source pollution in catchments upstream to the selected three locations in each river basin. We can see that, in most river basins, the amounts of both

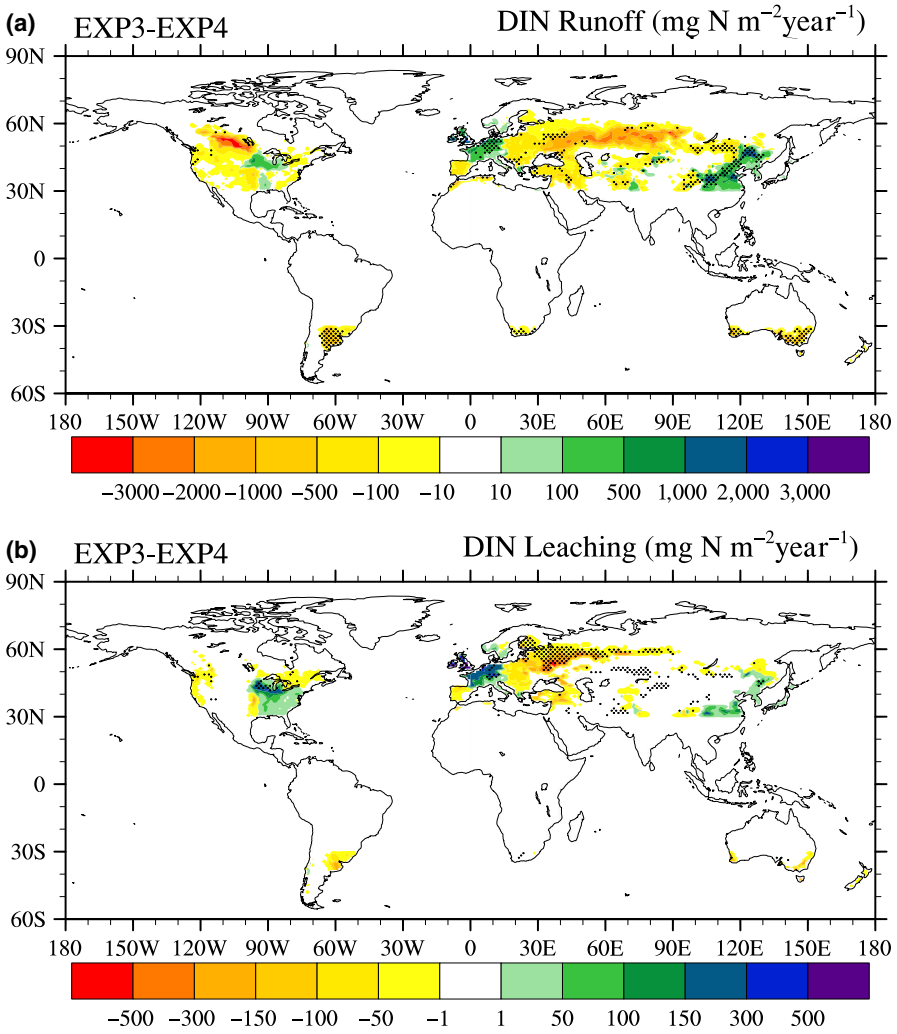

FIGURE 12 The 10-year averaged spatial distributions of the differences between EXP3 and EXP4 in terms of: (a) soil dissolved inorganic nitrogen (DIN) runoff and (b) soil DIN leaching. This picture shows the effects of different temperate fertilizer datasets on the DIN from the soil. The black dots indicate the regions where the difference passed the 95% confidence level of the Student's *t* test

the fertilizer usage and point source discharge were much bigger in the lower reaches, most of which were dominated by human societies. During the past 20 years, the annual amount of point source nitrogen pollution changed only a little in the Mississippi River Basin, the Rhine Basin, and the Danube Basin. The annual amount of fertilizer usage increased obviously in the Mississippi River Basin and the Yangtze River Basin. In the Mississippi River Basin, the total nitrogen fertilizer input for the whole basin increased from about 5–7 Tg. The input amounts of both nitrogen sources to the Yangtze River Basin increased. In this regard, the amount of point source pollution in 2010 was about four times greater than that in 1991, while the amount of fertilizer used in 2010 was about twice more than that in 1991. For this, the riverine DIN appropriately responded to human nitrogen input.

Figure 10 shows the mean annual DIN flow rate at the same sites mentioned above. First, we can see that the DIN flow rates simulated by EXP1 in the Mississippi River and the Yangtze River indicated slight downtrends, while that in the Ob River showed an increasing trend from 1991 to 2010. However, in the Yangtze River, the human nitrogen discharge gradually weaken the downtrend, as shown in Figure 10o. Combining the mean monthly and yearly results, we speculated that the riverine DIN in the USA was primarily affected by nitrogen fertilizer use, while the DIN flow rate in European rivers was primarily affected by point source pollution. Finally, the Yangtze River in China was polluted by both point source pollution and fertilizer use. In addition, during the crop-growing period, the use of nitrogen fertilizer played an important role in affecting the riverine DIN flow rate.

3.3 | Effects of anthropogenic nitrogen input on the DIN exported from rivers

Figure 11 shows the temporal changes in the modulatory levels of anthropogenic nitrogen discharge on the annual DIN exported from land to oceans over the period from 1991 to 2010. Figure 11a displays the changes in the effect of temperate fertilizer application. It shows that the impact on the DIN exported to the Pacific Ocean increased from 5% to 16%, while those for other three oceans did not change very much with time. It is suggested therefore that more densely populated regions contribute more nitrogen pollution to the oceans because of increased demand on grain yield, which in turn usually depends on sufficient fertilizer (Zhang et al., 2015). Figure 11b shows the changes in the impact of point source nitrogen pollution. We can see that the impact on the DIN exported to the

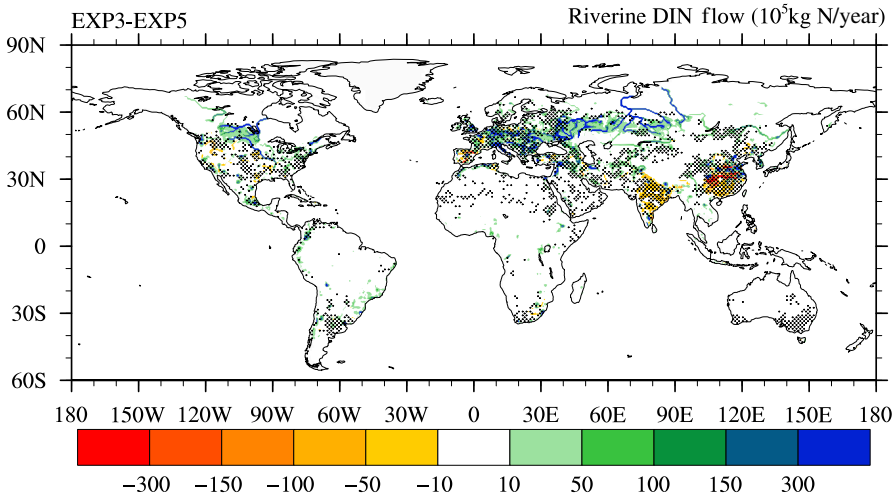

FIGURE 13 The 10-year averaged spatial distributions of the differences in the riverine dissolved inorganic nitrogen (DIN) flow rates between EXP3 and EXP5. This figure demonstrates the effects of anthropogenic nitrogen discharge and water regulations on the global riverine DIN flow rates. The black dots indicate the regions where the difference passed the 95% confidence level of the Student's *t* test

Pacific Ocean, Atlantic Ocean, and Indian Ocean always increased, from 4.5% to 12%, 6% to 8.5%, and 3% to 5%, respectively. It can be seen that the amount of point source nitrogen pollution on the riverine DIN in the Pacific region grew the most rapidly. Conversely, the impact on the DIN exported to the Arctic Ocean decreased, which may indicate that the annual point source pollution in the Arctic region gradually decreased during the 20-year period. Comparing the results from Figure 11a,b, we found that the impact of either fertilizer use or point source nitrogen discharge on the DIN exported to the Pacific Ocean rapidly increased. For the DIN exported to the other three oceans, the impact of fertilizer use was smaller than that of point source nitrogen discharge each year. Finally, from Figure 11c, the total anthropogenic nitrogen discharge largely affected the exported DIN, among which the impact on the DIN exported to the Pacific Ocean grew most significantly, from 10% to 30%.

3.4 | Limitations in this study

From the results and analyses, some differences exist between the simulated and observed values. The most likely reasons for these originate from both the uncertainties in the datasets and the model limitations.

From the aspect of data uncertainties, as the main input to nitrogen loading in rivers at a global scale, nitrogen fertilizer discharge had a large impact on the final calculation of the DIN runoff and leaching from the soil. The default amounts of fertilizer use in CLM4.5 were fixed for maize, temperate cereals, and soybeans, and they represented the amount the central USA uses for annual fertilizer application. In order to better embody the effects of fertilizer usage, we replaced the fixed data with the new dataset. Then, we conducted a supplementary sensitivity test with two groups of 10-year models to investigate how much the different fertilizer usage data affected the calculated DIN losses from the soil. From the 10-year averaged spatial patterns in Figure 12, we could see that different fertilizer usages resulted in some differences in both DIN runoff and leaching, which was especially significant in some regions of western Europe, Russia, and eastern China. After replacing the default data with the new data, the obvious increments in DIN runoff, which ranged from 500 to 3,000 mg m^{-2} $year^{-1}$, appeared in France, Germany, England, and China, while the most reduced amounts were in Russia, Canada and Uruguay. Meanwhile the DIN leaching decreased significantly in Russia and increased in northeast USA and western Europe.

In addition, we collected the observed DIN data from literature records for model validation. However, the observed data had uncertainties related to discharge measurements, sample collection, sample storage, and laboratory analysis (He et al., 2011). More importantly, the spatial scales of the observations and simulations were totally different. Hence, the model validation in this work may be not robust due to the uncertainties arising from both the model and the observed data. The collected observation data may only be used to prove the consistency at the "order-of-magnitude" level between the simulations and observations. Further model development and validation should be matched with an improved accuracy of observations.

From the aspect of model limitation, the current model development was based on CLM4.5, which includes only temperate-zone managed crops (Oleson et al., 2013). This means that crop growth with fertilizer in other latitude zones was not considered, so that the riverine nitrogen flow rates in some regions were likely underestimated. This problem should be addressed with further development of the BGC module in the land surface model. Although more types of crops in tropical regions in CLM5.0 could reduce some of the uncertainties discussed above, there were at least two aspects of model development that should also be further considered. The first is to simulate particulate and DON leaching flow rates in the CLM. The current lack of organic nitrogen leaching hinders direct comparisons of modeled and observed total nitrogen export. In addition, a recent study showed that even if agricultural N use became 100% efficient, it would take decades to meet target N loads due to legacy N within the Mississippi River basin. However, because it is indeed difficult to quantitatively describe for global rivers, presently we have not considered the conversion process of legacy N quantities (Van Meter, Cappellen, & Basu, 2018). The second is the

need to scrutinize the effects of water regulations on soil denitrification, leaching, and river nitrogen pollution. The ways in which surface water and groundwater use are different affect the soil nitrogen runoff and leaching differently. These related mechanisms may be useful for environmental protection from the perspective of water management.

As the riverine DIN transport is governed by river routing, any uncertainties in simulated river water flow will be translated into uncertainties in the simulated DIN transport. In this work, we made some modifications to the land and river hydrology in CLM4.5 and RTM. According to our early work (Xie et al., 2018; Zeng et al., 2017), we found that considering human water regulation could make the results of soil moisture, evaporation and river water flow more reasonable. Due to the large computing costs of running the BGC–BGP coupled system model, detailed tests of the effects of water regulation on land surface processes have not been done. Even so, a sensitivity test was conducted to help us understand the uncertainties related to the current results of water regulations in the model. Figure 13 shows the 10-year averaged combined effects of human nitrogen discharge and water regulations on the riverine DIN flow rates. It was still clear that the annual DIN flow rates in the temperate rivers increased, primarily due to fertilizer application. Conversely, the flow rates in other latitude zones, especially in the tropics and subtropics, decreased significantly due to the effects of water regulations. This was because only managed crops in temperate zones existed in the current version of CLM, but the schemes of global water regulations were incorporated. Moreover, the data on water use were estimated from statistical data at the country level, which were indeterminate in many local areas. Due to lack of consideration of the land cover changes, the spatial and temporal changes in the amounts of water use had more associated uncertainties. However, from a different perspective, it could be believed that the newly added schemes of riverine nitrogen transport and human activities in this work may be an effective tool to diagnose the performance of the land surface models and even the earth system models.

4 | CONCLUSIONS AND FUTURE PERSPECTIVES

In this work, we synchronously incorporated schemes related to global riverine DIN transport and human activities, including anthropogenic nitrogen discharge, and water regulation, into the land surface model CLM4.5. Using a series of data related to fertilizer application, point source pollution, surface water use, and groundwater use, numerical simulations for the period 1991–2010, which had a spatial resolution of 1° for land processes and 0.5° for river grid cells, were conducted for the entire world. The simulated riverine DIN flow rates had the same order of magnitude as observations obtained at 30 major world rivers, which loosely demonstrated the reliability of our developed model. The spatial patterns of the 20-year averaged results showed that after fertilizer application, the annual losses of soil DIN increased significantly, which further caused the riverine DIN to increase as well. The rivers in western Europe and eastern China were the most polluted, by rates of 5,000–15,000 tons per year, on average. During the past 20 years, the annual amount of fertilizer used increased obviously in the Mississippi River Basin and the Yangtze River Basin. In this regard, the amount of point source pollution in 2010 was about four times more than that in 1991, while the amount of fertilizer usage doubled in the Yangtze River Basin. The temporal changes in DIN flow rate in large rivers suggested that the riverine DIN in the USA was affected primarily by nitrogen fertilizer use. In turn, the changes in DIN flow rate in European rivers was dominated by point source pollution, and the Yangtze River in China was seriously polluted by both point source pollution and fertilizer use. The total anthropogenic nitrogen discharge largely affected the riverine DIN exports, among which the impact on the DIN exported to the Pacific Ocean grew significantly from 10% to 30% over the period from 1991 to 2010. In general, our results suggested that incorporating schemes related to riverine nitrogen transport and human activities into the model could be an effective way to monitor the global river water quality, and evaluate the performance of the global land surface modeling.

Apparently, although in this work we proposed and preliminarily implemented an integrated model framework to simulate the nitrogen transport from land to oceans, there are some shortcomings and problems. To thoroughly understand land–ocean nutrients transportation, we should advance the current model in some aspects. The first is to develop and integrate the parameterizations of the DIN conversion process between the river channel sediment or plants, and the fluid, which can reflect the effects of river legacy nitrogen on exported DIN. Then, in order to better reproduce the observation, we should globally tune the parameters in each process-based module after sufficiently incorporating essential parameterization schemes related to nitrogen transport, which is indeed difficult for more and more complex land surface or earth system models. The third is to replace the empirical and simple descriptions with mechanism-specific methods, which is helpful for attribution analyses. The fourth is to transplant the ideas of nitrogen transport into the new version of CLM, such as CLM5.0, which has a better river system model and includes more crop types in the BGC module. Once the model is validated well, it can be meaningful to reproduce the temporal variability of DIN export of all the global rivers for past tens of years. In addition, as an important component of the earth system models, in future work, the developed model in this work will be coupled with atmospheric and ocean models to simulate and project the global nitrogen cycle. Meanwhile, based on the fully coupled model, we may clearly differentiate the anthropogenic contributions to the environment and climate change.

ACKNOWLEDGEMENTS

This work was jointly supported by the Key Research Program of Frontier Sciences, Chinese Academy of Sciences (CAS) (grant number: QYZDY-SSW-DQC012) and by the National Natural Science Foundation of China (NSFC) project (grant number: 41830967 and 41575096). We

thank Dr. Hanasaki for providing us with the source code of the reservoir model. We would like to thank Junqiang Gao and Zhipeng Xie for their helpful discussion. We also thank the National Supercomputing Center of Tianjin, China for use of the supercomputer Tianhe-I.

CONFLICT OF INTEREST

The authors declare no competing financial interests.

ORCID

Shuang Liu https://orcid.org/0000-0003-1990-5574
Zhenghui Xie https://orcid.org/0000-0002-3137-561X
Jinbo Xie https://orcid.org/0000-0002-3003-9155

REFERENCES

Alexander, R. B., Böhlke, J. K., Boyer, E. W., David, M. B., Harvey, J. W., Mulholland, P. J., … Wollheim, W. M. (2009). Dynamic modeling of nitrogen losses in river networks unravels the coupled effects of hydrological and biogeochemical processes. *Biogeochemistry*, *93*, 91–116. https://doi.org/10.1007/s10533-008-9274-8

Andreadis, K. M., Schumann, G. J. P., & Pavelsky, T. (2013). A simple global river bankfull width and depth database. *Water Resources Research*, *49*, 7164–7168. https://doi.org/10.1002/wrcr.20440

Arnold, J. G., & Fohrer, N. (2005). SWAT2000: Current capabilities and research opportunities in applied watershed modelling. *Hydrological Processes*, *19*, 563–572. https://doi.org/10.1002/hyp.5611

Beek, L. P., Eikelboom, T., & Vliet, M. T., & Bierkens, M. F. (2012). A physically based model of global freshwater surface temperature. *Water Resources Research*, *48*, W09530. https://doi.org/10.1029/2012wr011819

Beusen, A., Bouwman, A., Dürr, H., & Dekkers, A., & Hartmann, J. (2009). Global patterns of dissolved silica export to the coastal zone: Results from a spatially explicit global model. *Global Biogeochemical Cycles*, *23*, *GB0A02*. https://doi.org/10.1029/2008GB003281

Beusen, A., Dekkers, A., Bouwman, A., Ludwig, W., & Harrison, J. (2005). Estimation of global river transport of sediments and associated particulate C, N, and P. *Global Biogeochemical Cycles*, *19*, GB4S05. https://doi.org/10.1029/2005GB002453

Beusen, A., Van Beek, L., Bouwman, A., Mogollón, J., & Middelburg, J. (2015). Coupling global models for hydrology and nutrient loading to simulate nitrogen and phosphorus retention in surface water–description of IMAGE–GNM and analysis of performance. *Geoscientific Model Development*, *8*, 4045–4067. https://doi.org/10.5194/gmd-8-4045-2015

Bouwman, A., Beusen, A. H., & Billen, G. (2009). Human alteration of the global nitrogen and phosphorus soil balances for the period 1970–2050. *Global Biogeochemical Cycles*, *23*, GB0A04. https://doi.org/10.1029/2009GB003576

Bouwman, A. F., Beusen, A., Overbeek, C., Bureau, D., Pawlowski, M., & Glibert, P. (2013). Hindcasts and future projections of global inland and coastal nitrogen and phosphorus loads due to finfish aquaculture. *Reviews in Fisheries Science*, *21*, 112–156. https://doi.org/10.1080/10641262.2013.790340

Bouwman, A. F., Pawłowski, M., Liu, C., Beusen, A. H., Shumway, S. E., Glibert, P., & Overbeek, C. (2011). Global hindcasts and future projections of coastal nitrogen and phosphorus loads due to shellfish and seaweed aquaculture. *Reviews in Fisheries Science*, *19*, 331–357. https://doi.org/10.1080/10641262.2011.603849

Boyer, E. W., Howarth, R. W., Galloway, J. N., Dentener, F. J., & Green, P. A., & Vörösmarty, C. J. (2006). Riverine nitrogen export from the continents to the coasts. *Global Biogeochemical Cycles*, *20*, GB1S91. https://doi.org/10.1029/2005GB002537

Branstetter, M. L., & Erickson III, D. J. (2003). Continental runoff dynamics in the community climate system model 2 (CCSM2) control simulation. *Journal of Geophysical Research*, *108*, 4550, https://doi.org/10.1029/2002JD003212, D17.

Drecht, G. V., Bouwman, A. F., Knoop, J. M., Beusen, A. H. W., & Meinardi, C. R. (2003). Global modeling of the fate of nitrogen from point and nonpoint sources in soils, groundwater, and surface water. *Global Biogeochemical Cycles*, *17*, 1115. https://doi.org/10.1029/2003GB002060

Galloway, J. N., Dentener, F. J., Capone, D. G., Boyer, E. W., Howarth, R. W., Seitzinger, S. P., …Vorösmarty, C. J. (2004). Nitrogen cycles: Past, present, and future. *Biogeochemistry*, *70*, 153–226. https://doi.org/10.1007/s10533-004-0370-0

Haddeland, I., Heinke, J., Biemans, H., Eisner, S., Flörke, M., Hanasaki, N., … Wisser, D. (2014). Global water resources affected by human interventions and climate change. *Proceedings of the National Academy of Sciences*, *111*, 3251–3256. https://doi.org/10.1073/pnas.1222475110

Hanasaki, N., Kanae, S., & Oki, T. (2006). A reservoir operation scheme for global river routing models. *Journal of Hydrology*, *327*, 22–41. https://doi.org/10.1016/j.jhydrol.2005.11.011

Hao, H., Li, K., & Zhuang, C. (2005). Study on 1-D water temperature forecast model of river unsteady flow. *Journal of Sichuan University (Natural Science Edition)*, *42*, 1189–1193.

Harison, J., Seitzinger, S., Bouwman, A., Caraco, N., & Beusen, A., & Vörösmarty, C. J. (2005). Dissolved inorganic phosphorus export to the coastal zone: Results from a spatially explicit, global model. *Global Biogeochemical Cycles*, *19*, GB4S03. https://doi.org/10.1029/2004GB002357

He, B., Kanae, S., Oki, T., Hirabayashi, Y., Yamashiki, Y., & Takara, K. (2011). Assessment of global nitrogen pollution in rivers using an integrated biogeochemical modeling framework. *WaterResearch*, *45*, 2573–2586. https://doi.org/10.1016/j.watres.2011.02.011

Howarth, R. W. (1998). An assessment of human influences on fluxes of nitrogen from the terrestrial landscape to the estuaries and continental shelves of the North Atlantic Ocean. *Nutrient Cycling in Agroecosystems*, *52*, 213–223.

Hurrell, J. W., Holland, M. M., Gent, P. R., Ghan, S., Kay, J. E., Kushner, P. J., … Marshall, S. (2013). The community earth system model: A framework for collaborative research. *Bulletin of the American Meteorological Society*, *94*, 1339–1360. https://doi.org/10.1175/BAMS-D-12-00121.1

Jickells, T. (1998). Nutrient biogeochemistry of the coastal zone. *Science*, *281*, 217–222. https://doi.org/10.1126/science.281.5374.217

Lindsay, K., Bonan, G. B., Doney, S. C., Hoffman, F. M., Lawrence, D. M., Long, M. C., … Thornton, P. E. (2014). Preindustrial-control and twentieth-century carbon cycle experiments with the Earth System Model CESM1 (BGC). *Journal of Climate*, *27*, 8981–9005. https://doi.org/10.1175/JCLI-D-12-00565.1

Lu, C., & Tian, H. (2017). Global nitrogen and phosphorus fertilizer use for agriculture production in the past half century: Shifted hot spots and nutrient imbalance. *Earth System Science Data*, *9*, 181. https://doi.org/10.5194/essd-9-181-2017

Maavara, T., Parsons, C. T., Ridenour, C., Stojanovic, S., Dürr, H. H., Powley, H. R., & Van Cappellen, P. (2015). Global phosphorus retention by river damming. *Proceedings of the National Academy of Sciences*, *112*, 15603–15608. https://doi.org/10.1073/pnas.1511797112

Mayorga, E., Seitzinger, S. P., Harrison, J. A., Dumont, E., Beusen, A. H. W., Bouwman, A. F., … Van Drecht, G. (2010). Global nutrient export from WaterSheds 2 (NEWS 2): Model development and implementation. *Environmental Modelling & Software*, *25*, 837–853. https://doi.org/10.1016/j.envsoft.2010.01.007

Mitchell, T. D., & Jones, P. D. (2005). An improved method of constructing a database of monthly climate observations and associated high-resolution grids. *International Journal of Climatology*, *25*, 693–712. https://doi.org/10.1002/joc.1181

Morée, A., Beusen, A., Bouwman, A., & Willems, W. (2013). Exploring global nitrogen and phosphorus flows in urban wastes during the twentieth century. *Global Biogeochemical Cycles*, *27*, 836–846. https://doi.org/10.1002/gbc.20072

Nevison, C., Hess, P., Riddick, S., & Ward, D. (2016). Denitrification, leaching, and river nitrogen export in the Community Earth System Model. *Journal of Advances in Modeling Earth Systems*, *8*, 272–291. https://doi.org/10.1002/2015ms000573

Oleson, K. W., Lawrence, D. M., Bonan, G. B., Drewniak, B., Huang, M., Koven, C. D., … Yang, Z.-L. (2013). *Technical description of version 4.5 of the community land model (CLM)*. Ncar Technical Note NCAR/TN-503+STR, Boulder, CO: National Center for Atmospheric Research, 422 pp.

Peierls, B. L., Caraco, N. F., Pace, M. L., & Cole, J. J. (1991). Human influence on river nitrogen. *Nature*, *350*, 386–387. https://doi.org/10.1038/350386b0

Piao, S., Ito, A., Li, S., Huang, Y., Ciais, P., Wang, X. H., … Zhu, B. (2012). The carbon budget of terrestrial ecosystems in East Asia over the last two decades. *Biogeosciences*, *9*, 3571–3586. https://doi.org/10.5194/bg-9-3571-2012

Pokhrel, Y. N., Hanasaki, N., Wada, Y., & Kim, H. (2016). Recent progresses in incorporating human land–water management into global land surface models toward their integration into Earth system models. *Wiley Interdisciplinary Reviews: Water*, *3*, 548–574. https://doi.org/10.1002/wat2.1150

Raptis, C. E., & Pfister, S. (2016). Global freshwater thermal emissions from steam-electric power plants with once-through cooling systems. *Energy*, *97*, 46–57. https://doi.org/10.1016/j.energy.2015.12.107

Seitzinger, S., Harrison, J., Dumont, E., Beusen, A. H., & Bouwman, A. (2005). Sources and delivery of carbon, nitrogen, and phosphorus to the coastal zone: An overview of Global Nutrient Export from Watersheds (NEWS) models and their application. *Global Biogeochemical Cycles*, *19*, GB4S01. https://doi.org/10.1029/2005GB002606

Seitzinger, S., Mayorga, E., Bouwman, A., Kroeze, C., Beusen, A. H. W., Billen, G., … Harrison, J. A. (2010). Global river nutrient export: A scenario analysis of past and future trends. *Global Biogeochemical*, *Cycles*, 24. https://doi.org/10.1029/2009GB003587

Seitzinger, S. P., & Phillips, L. (2017). Nitrogen stewardship in the Anthropocene. *Science*, *357*, 350–351. https://doi.org/10.1126/science.aao0812

Siebert, S., Henrich, V., Frenken, K., & Burke, J. (2013). *Update of the digital global map of irrigation areas to version 5*. Rheinische Friedrich-Wilhelms-Universität, Bonn, Germany and Food and Agriculture Organization of the United Nations, Rome, Italy. Retrieved from https://www.lap.uni-onn.de/research/downloads/gmia/siebert_et_al_2013_gmia5/

Van Cappellen, P., & Maavara, T. (2016). Rivers in the Anthropocene: Global scale modifications of riverine nutrient fluxes by damming. *Ecohydrology & Hydrobiology*, *16*, 106–111. https://doi.org/10.1016/j.ecohyd.2016.04.001

Van Meter, K. J., Van Cappellen, P., & Basu, N. B. (2018). Legacy nitrogen may prevent achievement of water quality goals in the Gulf of. *Mexico. Science*, *360*, 427–430. https://doi.org/10.1126/science.aar4462

Van Vliet, M. T., Franssen, W. H., Yearsley, J. R., Ludwig, F., Haddeland, I., Lettenmaier, D. P., & Kabat, P. (2013). Global river discharge and water temperature under climate change. *Global Environmental Change*, *23*, 450–464. https://doi.org/10.1016/j.gloenvcha.2012.11.002

Van Vliet, M., Ludwig, F., Zwolsman, J., Weedon, G., & Kabat, P. (2011). Global river temperatures and sensitivity to atmospheric warming and changes in river flow. *Water Resources Research*, *47*, W02544. https://doi.org/10.1029/2010WR009198

Van Vliet, M., Yearsley, J., Franssen, W., Ludwig, F., Haddeland, I., Lettenmaier, D., & Kabat, P. (2012). Coupled daily streamflow and water temperature modelling in large river basins. *Hydrology and Earth System Sciences*, *16*, 4303–4321. https://doi.org/10.5194/hess-16-4303-2012

Viovy, N. (2011). CRUNCEP dataset. [Description available at . Data available at http://dods.extra.cea.fr/data/p529viov/cruncep/readme.htmhttp://dods.extra.cea.fr/store/p529viov/cruncep/V4_1901_2011/]

Woli, P., Hoogenboom, G., & Alva, A. (2016). Simulation of potato yield, nitrate leaching, and profit margins as influenced by irrigation and nitrogen management in different soils and production regions. *Agricultural Water Management*, *171*, 120–130. https://doi.org/10.1016/j.agwat.2016.04.003

Wollheim, W. M., Peterson, B. J., Thomas, S. M., & Hopkinson, C., & Vörösmarty, C. (2008). Dynamics of N removal over annual time periods in a suburban river network. *Journal of Geophysical Research*, *113*, G03038 and GB2026. https://doi.org/10.1029/2007jg000660

Wollheim, W. M., Vörösmarty, C. J., Bouwman, A., Green, P., Harrison, J., Linder, E., … Syvitski, J. P. M. (2008). Global N removal by freshwater aquatic systems using a spatially distributed, within-basin approach. *Global Biogeochemical Cycles*, *22*, GB2026. https://doi.org/10.1029/2007gb002963

Wunderlich, W. O., & Gras, R. (1967). *Heat and mass transfer between a water surface and the atmosphere*. Norris, TN: Tennessee Valley Authority, Division of Water Cont. Planning.

Xie, Z., Liu, S., Zeng, Y., Gao, J., Qin, P., Jia, B., … Wang, L. (2018). A high-resolution land model with groundwater lateral flow, water use, and soil freeze-thaw front dynamics and its applications in an endzorheic Basin. *Journal of Geophysical Research: Atmospheres*, *123*, 7204–7222. https://doi.org/10.1029/2018JD028369

Xu, X., Yu, J., Li, H., & Yang, L. (2016). Comparative study on calculation methods of dew-point temperature. *Journal of Meteorology and Environment*, *32*, 107–111.

Zeng, Y., Xie, Z., Yu, Y., Liu, S., Wang, L., Zou, J., … Jia, B. (2016). Effects of anthropogenic water regulation and groundwater lateral flow on land processes. *Journal of Advances in Modeling Earth Systems*, *8*, 1106–1131. https://doi.org/10.1002/2016MS000646

Zeng, Y., Xie, Z., & Zou, J. (2017). Hydrologic and climatic responses to global anthropogenic groundwater extraction. *Journal of Climate*, *30*, 71–90. https://doi.org/10.1175/JCLI-D-16-0209.1

Zhang, X., Davidson, E. A., Mauzerall, D. L., Searchinger, T. D., Dumas, P., & Shen, Y. (2015). Managing nitrogen for sustainable development. *Nature*, *528*, 51. https://doi.org/10.1038/nature15743

Zou, J., Xie, Z., Yu, Y., Zhan, C., & Sun, Q. (2014). Climatic responses to anthropogenic groundwater exploitation: A case study of the Haihe River Basin, Northern China. *Climate Dynamics*, *42*, 2125–2145. https://doi.org/10.1007/s00382-013-1995-2

Zou, J., Xie, Z., Zhan, C., Qin, P., Sun, Q., Jia, B., & Xia, J. (2015). Effects of anthropogenic groundwater exploitation on land surface processes: A case study of the Haihe River Basin, northern China. *Journal of Hydrology*, *524*, 625–641. https://doi.org/10.1016/j.jhydrol.2015.03.026

SUPPORTING INFORMATION

Additional supporting information may be found online in the Supporting Information section at the end of the article.

How to cite this article: Liu S, Xie Z, Zeng Y, et al. Effects of anthropogenic nitrogen discharge on dissolved inorganic nitrogen transport in global rivers. *Glob Change Biol*. 2019;00:1–21. https://doi.org/10.1111/gcb.14570